Comparative Medicine
Copyright 2021
by the American Association for Laboratory Animal Science

Vol 71, No 1
February 2021
Pages 46–65

Original Research

Comparison of Effects of *Trichuris muris* and Spontaneous Colitis on the Proximal Colon Microbiota in C3H/HeJ and C3Bir IL10$^{-/-}$ Mice

Jamie J Kopper,[1,5,6] Kevin R Theis,[3] Nicholas I Barbu,[1,5] Jon S Patterson,[4,5] Julia A Bell,[1,2,5] Jenna R Gettings,[1] and Linda S Mansfield[1–3,5,*]

The nematode *Trichuris muris* has been shown to interact with specific enteric bacteria, but its effects on the composition of its host's microbial community are not fully understood. We hypothesized that *Trichuris muris*-infected mice would have altered colon microbiota as compared with uninfected mice. Colon histopathology and microbial community structure and composition were examined in mouse models of colitis (C3BirTLR4$^{-/-}$ IL10$^{-/-}$ and C3H/HeJ TLR4$^{-/-}$ IL10$^{+/+}$ mice) with and without *T. muris* infection, in uninfected C3BirIL10$^{-/-}$ mice with and without spontaneous colitis, and in normal C3H/HeJ mice. *T. muris*-infected mice developed colon lesions that were more severe than those seen in IL10-deficient mice. Approximately 80% of infected IL10$^{-/-}$ mice had colon neutrophilic exudates, and some had extraintestinal worms and bacteria. The composition and structure of proximal colon microbiota were assessed by using terminal restriction fragment length polymorphism analysis targeting the bacterial 16S rRNA gene. Colon microbiota in C3BirIL10$^{-/-}$ and C3H/HeJ mice differed both qualitatively and quantitatively. *Trichuris* infection significantly altered the relative abundance of individual operational taxonomic units [OTU] but not the composition (presence or absence of OTU) of colon microbiota in the 2 mouse genotypes. When C3BirIL10$^{-/-}$ and C3H/HeJ mouse OTU were considered separately, *Trichuris* was found to affect the microbiota of C3BirIL10$^{-/-}$ mice but not of C3H/HeJ mice. Even though 34 of the 75 (45%) C3BirIL10$^{-/-}$ mice had spontaneous colitis, neither qualitative nor quantitative differences were detected in microbiota between colitic or noncolitic C3BirIL10$^{-/-}$ mice or noncolitic C3H/HeJ mice. Therefore, *Trichuris*-infected mice developed distinct microbial communities that were influenced by host background genes; these alterations cannot be attributed solely to colonic inflammation.

Abbreviations: ANOSIM, analysis of similarities; C3Bir IL10$^{-/-}$, C3Bir.129P2(B6)-IL10$^{-/-}$mice; Cdcs 1, cytokine deficiency colitis susceptibility 1 allele; ESP, excretory secretory products; ICC–J, ileocecocolic junction; MiCA, microbial community analysis; NMDS, nonmetric multidimensional scaling; UPGMA, unweighted pair group method with arithmetic averaging; OTU, operational taxonomic unit; qPCR, quantitative real-time PCR; SIMPER, similarity percentage; T-RFLP, terminal restriction fragment length polymorphism

DOI: 10.30802/AALAS-CM-20-000021

Trichuris spp. are gastrointestinal nematodes that dwell in close association with a complex bacterial community in the host's colon. After ingestion, embryonated eggs hatch in the cecum or colon releasing first-stage larvae that penetrate the epithelium and undergo 4 molts before becoming sexually mature. Both larval and adult *Trichuris* form syncytial tunnels in the colonic epithelium[21,30] that anchor the organisms in the proximal colon, where females produce eggs that pass in feces and embryonate in the environment.

Received: 06 Mar 2020. Revision requested: 06 May 2020. Accepted: 05 Aug 2020.
[1]Comparative Enteric Diseases Laboratory; Departments of [2]Large Animal Clinical Sciences, [3]Microbiology and Molecular Genetics, and [4]Pathobiology and Diagnostic Investigation; [5]College of Veterinary Medicine, Michigan State University, East Lansing, Michigan; and [6]Cell and Molecular Biology Program, College of Natural Science, Michigan State University, East Lansing, Michigan
[*]Corresponding author. Email: mansfie4@cvm.msu.edu

T. suis excretory secretory products (ESP) condition the colonic environment for enhanced worm survival, including effects on intestinal bacteria. Previous work demonstrated that *T. suis* ESP had dose-dependent effects on the tight junctions of epithelial cells.[1] The ESP fraction below a molecular weight of 10,000 kDa was mainly composed of an antimicrobial moiety[2] with bactericidal activity against gram-negative (*Campylobacter jejuni*, *C. coli*, and *Escherichia coli*) and gram-positive (*Staphylococcus aureus*) bacteria. In addition, due to several enzymatic activities, *T. suis* ESP have been demonstrated to aid the worms in burrowing into the host's colonic epithelium and in feeding.[1,10,12] In addition to a 20-kDa diagnostic antigen,[10,11] higher molecular-weight fractions of ESP harbored a 42-kDa zinc metalloprotease that likely functions to provide nutrition for the worms through collagenase and elastase activities.[10] Furthermore, a serine protease inhibitor (TsCEI) was purified from adult-stage *T. suis* by using acid precipitation, affinity chromatography, and

reverse-phase HPLC.[33] This 6.43-kDa TsCEI inhibited chymotrypsin, pancreatic elastase, neutrophil elastase, and cathepsin G and was suggested to function as a parasite defense mechanism by modulating host immune responses. Indeed, exposure of cultured epithelial cells to *T. suis* ESP elicited IL6 and IL10 cytokine responses.[31]

Trichuris has also been reported to interact with bacteria in vivo. Early studies demonstrated development of diarrhea in weaning age pigs concurrently harboring *T. suis* and various bacteria.[35] A mixed inoculum of *T. suis* and cecal scrapings containing *Brachyspira*, *Campylobacter* spp., or *Salmonella* spp. were implicated in this diarrhea by means of passive transfer to SPF pigs.[35] Interactions between this helminth and enteric bacteria were also explored by antibiotic treatment of *T. suis*-infected pigs.[20,27] Results of both passive transfer and antibiotic treatment experiments in pigs showed that *Trichuris* and various bacterial strains were necessary to produce the type of diarrhea and colonic lesions seen in weaning aged pigs in production, but did not implicate a single bacterial agent. In 2003, synergism between *T. suis* and *C. jejuni* was proven to cause mucohemorrhagic colitis in that germ-free piglets inoculated with both agents developed disease, whereas those infected with a single agent did not.[25] Recent studies in *T. suis*-infected pigs show changes in the microbial community of the colon with some accompanying metabolic changes.[22,45] Similar interactions have been found in extensive studies of captive rhesus monkeys with chronic enterocolitis. In these monkeys, severe disease was associated with presence of *Trichuris trichiura* and several enteric pathogens including *C. coli*, *C. jejuni*, *Shigella flexneri*, *Yersinia enterocolitica*, adenovirus, and *Strongyloides fulleborni*.[38] Therefore, *Trichuris* interacts with and may demonstrate synergy in disease production with the host's colonic microflora.

Interactions between *Trichuris* and bacteria have also been studied in mice.[9,20,36] One study found 100% morbidity in C57BL/6 IL10$^{-/-}$ and congenic IL10$^{-/-}$ IL4$^{-/-}$ mice after challenge with *T. muris*.[36] The authors hypothesized that this high morbidity was due to an overgrowth of opportunistic invasive bacteria that use the mechanical damage caused by *T. muris* larvae to breach the intestinal tract. Adding the broad-spectrum antibiotic neomycin sulfate to the drinking water of IL10$^{-/-}$ IL4$^{-/-}$ mice and then infecting them with *T. muris* resulted in a statistically significant increase in the percentage of mice that survived infection.[36] The authors concluded that growth of opportunistic bacteria may have contributed to the previously observed morbidity and mortality. Most recently, another group[9] found that increased levels of colonic microflora favor increased numbers of *T. muris* and chronic infections. The group also demonstrated that *T. muris* eggs hatched more efficiently in vitro when incubated with explants of mouse cecum containing 5 isolates of bacteria (*E. coli, Staphylococcus aureus, Salmonella typhimurium*, or *Pseudomonas aeruginosa*) and the yeast *Saccharomyces cerevisiae,* with the greatest effects seen at 37 °C. Similarly, work from our laboratory[20] demonstrated that treatment of *T. muris*-infected C57BL/6 IL10$^{-/-}$ mice with metronidazole but not prednisolone increased survival.[20] Most recently, chronic infections with *T. muris* in C57BL/6 mice have been shown to decrease the diversity of intestinal microbiota,[13] increase the abundance of *Lactobacillus* spp., and alter the metabolome.[14]

Taken together, these data suggest an important microbial component to the pathogenesis of *Trichuris* infections in a variety of species. Given that *Trichuris suis* has been administered to patients with inflammatory bowel disease (IBD), and in some studies appeared to diminish IBD symptoms[42,43] we sought to understand the community-wide interactions of this worm with enteric bacteria in a mouse model of colitis. We hypothesized that the microbiota of the proximal colon would differ significantly in mice infected with *T. muris* as compared with uninfected mice. We theorized that these effects would occur due to the worm's immunomodulatory properties in the host and may contribute to the successful outcomes of *Trichuris* treatment in patients with IBD.

Materials and Methods

Mouse genetic background, breeding, and handling. All animal protocols were approved by the Michigan State University IACUC and complied with the *Guide for the Care and Use of Laboratory Animals*[16] and NIH guidelines (04/07-044-00). Briefly, C3H/HeJ TLR4$^{-/-}$ IL10$^{+/+}$ (referred to throughout as C3H/HeJ) and C3Bir.129P2(B6)-IL10$^{-/-}$ (referred to throughout as C3BirIL10$^{-/-}$) mice were obtained from barrier facilities at The Jackson Laboratories (Bar Harbor, ME). Previously, one group of investigators had documented a role for the cytokine deficiency colitis susceptibility (Cdcs1) gene product(s) in these mice in the development of spontaneous colitis in C3BirIL10$^{-/-}$ but not C3H/HeJ mice.[4,5] We confirmed this finding in experimental infections with a colitogenic strain of *C. jejuni*.[26] Breeding, genotyping of mice, and testing for enteric pathogens (*Helicobacter* spp., *Campylobacter* spp., *Citrobacter rodentium*, *Enterococcus faecalis*, and *Enterococcus faecium*) both prior to and at the conclusion of the experiment were performed as previously described.[24]

Dedicated C3BirIL10$^{-/-}$ sentinel mice were used to monitor for bacterial, protozoal, and viral agents throughout our institution's Laboratory Animal Resources Facility, both in the breeding colony and at our Research Containment Facility. We also monitored the mouse colony for the incidence of spontaneous colitis by examining euthanized retired breeding mice and examined mice euthanized for other reasons for enlargement of the proximal colon, cecum, ileocecocolic junction (ICC–J) lymph node, and spleen. The feces of mice that exhibited signs of colitis were screened for the presence of the known colitis-causing bacteria (previously mentioned), by using DNA isolated from proximal colon samples.[24]

When designated experimental mice reached the age of 8 to 12 wk, they were transported to the Research Containment Facility in autoclaved polycarbonate filter-topped cages in sterile dog crates for use in experiments. All mice were housed individually in autoclaved polycarbonate filter-topped cages (Ancare, Bellmore, NY) on sterile rolled paper bedding, fed irradiated 7904 mouse breeder diet (Harlan Teklad, Indianapolis, IN), given autoclaved water and autoclaved cotton squares, and randomly assigned by random number generator (www.random.org) to cage locations on the racks without regard to genetic background or treatment group. In experiment 2, C3BirIL10$^{-/-}$ and C3H/HeJ mice that were used to assess the incidence of spontaneous colitis remained within our barrier breeding colony for the entirety of the experiment. Their husbandry was the same as for mice in experiment 1.

Parasites. *T. muris* eggs of the J isolate were originally obtained from Dr Joseph Urban (USDA, Beltsville, MD) and used to infect SCID mice to obtain adult *T. muris* worms. Egg stocks were collected and stored as previously described.[19] The stocks were monitored by microscopy for the presence of fungal or bacterial infection and discarded if contamination was detected.

Parasite inoculum preparation and infection. *Trichuris muris* egg inoculum was prepared as previously described.[19] Briefly, eggs were surface-sterilized by using 6.25% hypochlorite (bleach) and washed in sterile PBS. Infectivity and viability were confirmed by using propidium iodide staining and in vitro

hatching assays. Mice were gavaged with embryonated *T. muris* eggs in 200 µL PBS according to experimental group assignment, by using 1-mL tuberculin syringes with sterile 22-gauge curved stainless steel feeding needles.

Experimental design. In experiment 1, 10 or 11 C3H/HeJ and C3BirIL10$^{-/-}$ mice were divided into randomized age- and sex-matched experimental groups, resulting in 5 or 6 mice of both strains per group. Each mouse received 100 embryonated *T. muris* eggs or sham inoculations orally, as designated (Table 1). This sample size was chosen to assure sufficient power to detect differences in the gut microbiome even though no data were available at this time. Mice with clinical signs of disease were euthanized prior to the scheduled necropsy if required for humane reasons, based on our scoring system for clinical signs of disease.[24] All remaining mice were euthanized 40 d after infection. This 40-d experimental end-point was chosen based on data from a previous mouse experiment that showed the presence of adult worms and patency with peak egg-shedding in fecal pellets at this time.[19] For statistical analyses of enteric and extraintestinal lesions according to histologic scoring, mice were divided into early (before day 29) and late (after day 29) groups.

In experiment 2, C3BirIL10$^{-/-}$ mice were used to assess the development of spontaneous colitis within the breeding colony. Mice were monitored daily for clinical signs associated with colitis, by using a case–control design. Mice with colitis were euthanized if clinical signs reached humane endpoints according to an approved score sheet designed to prevent animal suffering.[24] At the same times, noncolitic C3BirIL10$^{-/-}$ and C3H/HeJ mice of similar age and sex were euthanized to serve as controls for those with spontaneous colitis (Table 2).

Monitoring of experimentally infected mice for clinical signs. Mice were evaluated for clinical signs of disease 1 to 4 times daily by a trained observer using a standardized score sheet.[24] The frequency of monitoring increased with the severity of the clinical score. Briefly, mice were monitored for clinical signs including, but not limited to, rough hair coat, hunched posture, decreased activity, diarrhea, dehydration, increased respiration rate, and signs of shock. Each factor, when present, received a numerical score, with higher scores for more severe clinical signs of disease. Any mouse receiving a score of 8 or above was immediately euthanized and necropsied. This method allowed us to identify animals in the early stages of disease in a standardized manner.

Methods for necropsy, gross pathology, and histopathology. Mice were euthanized by CO_2 overdose consistent with AVMA guidelines[3] and weighed. Prior to opening the gastrointestinal tract, spleens were removed aseptically, weighed, and cut on the sagittal plane. One half of the tract was infused with Carnoy solution, placed in a histologic cassette (Histocette II, Simport Plastics, Beloeil, Quebec, Canada), and submerged in Carnoy solution for 24 h; the fixative was then decanted and the tissue placed in 60% ethanol. The other half was snap-frozen by using dry ice for subsequent DNA extraction. The gastrointestinal tract was removed in its entirety to absorbent Versi-Dry paper (Nalgene, Rochester, NY) to prevent cross-contamination of the samples. Gross pathologic changes were noted and photographed. Changes seen included enlargement of the ICC–J and mesenteric lymph nodes, thickening of the wall of the gastrointestinal tract, and distention of the gastrointestinal tract lumen with fluid or bloody contents. Care was taken to avoid contaminating the serosal surfaces with either *T. muris* or intestinal contents. A 0.5-cm cross-section of colon was sectioned by using sterile scissors and snap-frozen in a cryovial for terminal restriction fragment length polymorphism (T-RFLP) microbial community studies. The cecum with approximately 1 cm of both the terminal ileum and proximal colon was placed on a sponge in a histologic cassette, immediately injected with Carnoy solution, and submerged in Carnoy solution for 24 h. Thereafter, the fixative was decanted and the cassette placed in 60% ethanol in preparation for histologic analysis. All Carnoy-fixed tissues stored in ethanol were embedded in paraffin and cut in 5 µm sections. One section was stained with hematoxylin and eosin and another section was Gram stained at the Investigative Histopathology Laboratory (Division of Human Pathology, Department of Physiology, Michigan State University). Sections were observed and photographed by using a Nikon Eclipse E600 microscope with a SPOT camera and Windows version 4.09 software (RT-Slider Diagnostic Instruments, Sterling Heights, MI).

Scoring of histopathologic lesions. The scoring system used to evaluate histopathologic changes in the ICC–J of each mouse assigned numerical grades based on severity, as previously reported.[24] The lumen was evaluated for excess mucus and inflammatory exudates; the epithelium for surface integrity, number of intraepithelial lymphocytes, goblet cell hypertrophy, goblet cell depletion, crypt hyperplasia, crypt atrophy and crypt inflammation; the lamina propria and submucosa for increases in inflammatory or immune cells and changes in the distribution of those cells; and the submucosa for fibrosis, inflammatory cells and edema. All histologic sections were scored by 2 individuals (JJK and JSP, a board-certified pathologist) who were blind to the identities and experimental groups of mice. In the few slides for which scoring discrepancies occurred, the 2 scorers reviewed the slides together and selected a single score for each category. Spleen sections were scored by a single observer (JJK) who used separate standardized scoring criteria that graded the size of periarteriolar sheaths, degree of extramedullary hematopoiesis, and the amount of mononuclear lymphocyte infiltration.[26]

DNA extraction and T-RFLP analysis. DNA was extracted from frozen proximal colon tissue samples by using a DNeasy tissue kit (QIAgen, Valencia, CA) according to the manufacturer's instructions. Each DNA sample was used as the template for the 16S rRNA gene universal primers 5′-fluorescent (6-FAM)′-TGC CAG CAG CCG CGG TA-3′ (516f) and 5′-GGT TAC CTT GTT ACG ACT T-3′ (1510r), in a reaction mixture described previously[29] and with the following modifications: (1) the total amount of sample DNA was increased to 400 ng per 50-µL reaction, (2) 25 pM of primers was used per 50-µL reaction, (3) the annealing time was increased to 60 s and (4) the elongation time was increased to 120 s. Two 50-µL reactions were combined for each mouse sample.

In preliminary trials, T-RFLP OTU from 3 different restriction enzyme digests were compared, and each combination of T-RFLP operational taxonomic units (OTU; *Hae*III–*Bsl*I, *Hae*III–*Msp*I, *Msp*I–*Bsl*I, and *Hae*III–*Bs*lI–*Msp*I) was evaluated to determine whether the additional fragments from other restriction digests would increase the sensitivity of the analysis. TRFLP peaks with a height of 50 fluorescent units or greater were included in the analyses and reported as fragment-size OTU. For restriction enzyme combination analyses, the OTU from each independent restriction enzyme digest were analyzed together. PAST software was used for multivariate analysis of similarities (ANOSIM) and cluster analyses for visual representation.[8] Samples were analyzed by comparing both the presence and absence and the relative abundance of OTU according to Jaccard and Bray–Curtis similarity indices, respectively. N was equal to 10,000 permutations for all analyses. In ANOSIM, the statistical null hypothesis that samples were derived from the same community was rejected when the *P* value was 0.05 or less. Only

Table 1. Experimental design for the study of the effect of *T. muris* on proximal colon microbiota. Mice were given either 100 embryonated *T. muris* eggs (infected) or were given PBS as a sham inoculation (uninfected). Groups were age and sex matched.

Experimental group	C3H/HeJ (male, female)	C3Bir IL10$^{-/-}$ (male, female)
Infected	10 (5,5)	11 (6,5)
Uninfected	9 (5,4)	11 (5,6)

Table 2. Experimental design for the study of colonic microbiota in C3Bir IL-10$^{-/-}$ mice with and without clinical signs of spontaneous colitis and C3H/HeJ controls. At the time of euthanasia of mice with colitis, a clinically normal mouse that was similar in terms of age and sex was also euthanized as a comparison when available.

Experimental group	C3Bir IL10$^{-/-}$Total (male, female)	C3H/HeJ Total (male, female)
Spontaneous colitis	28 (11, 17)	0 (0,0)
Noncolitic	21 (13, 8)	12 (7, 5)

Table 3. Summary of qPCR Primer Sequences

Target bacteria	Forward (5′-3′)	Reverse (5′-3′)
Bacteroides spp.[31]	GGTGTCGGCTTAAGTGCCAT	CGGA(C/T)GTAAGGGCCGTGC
E. coli[15]	CAATTTTCGTGTCCCCTTCG	GTTAATGATAGTGTGTCGAAA
Clostridium Group I[31]	CGGTACCTGACTAAGAAGC-	AGTTT(C/T)ATTCTTGCGAACG
Clostridium Group XIV[31]	ATGCAAGTCGAGCGA(G/T)G	TATGCGGTATTAATCT(C/T)CCTT

minor differences were detected in the *P* (same) and R values between different analyses of individual restriction enzymes and their combinations. Therefore, for both experiments 1 and 2, the combined product of the two 50-µL reactions was digested with *Bsl*I (New England Biolabs, Ipswich MA) according to the manufacturer's instructions and purified by using QIAQuick PCR Purification Columns (QIAgen). Samples were submitted to our institution's Research Technology Support Facility for T-RFLP analysis. DNA samples from 2 C3Bir IL10$^{-/-}$ infected mice, 3 C3Bir IL10$^{-/-}$ uninfected mice, and one mouse each from the infected and uninfected C3H/HeJ groups repeatedly failed to yield 16S rRNA PCR products due to low DNA template yields and were not included in T-RFLP analyses.

Quantitative real-time PCR (qPCR) analysis. DNA extracted from the proximal colon lumen and tissue-associated contents as previously described[34] was used as the template in species-specific qPCR assays. *Clostridium* groups I and XIV and *Bacteroides* assays were performed by using previously described primer sequences.[34] *Escherichia coli* qPCR assays were performed by using other appropriate primer sequences.[17] Primer sequences are summarized in Table 3. In all assays, 25-µL reactions were performed in triplicate for each sample by using SYBR Green PCR master mix (Applied Biosystems, Foster City, CA), 12.5 pM of bacterial specific primers, and 50 ng of sample DNA. All qPCR assays included a 7-point standard curve run in triplicate ($R^2 > 0.90$) and 3 nontemplate controls containing all other reaction components. qPCR data were analyzed by using a Bio-Rad iQ5 Real-Time PCR Detection System (Bio-Rad, Hercules).

Statistical analyses. *Analysis of histologic scoring of ICC–J and spleen.* Preliminary analyses of histopathologic scoring data were conducted by using Kruskal–Wallis nonparametric one-way ANOVA as previously described.[24] When the result indicated that statistically significant differences existed among groups in an analysis, pairwise comparisons between groups were conducted by using the Fisher exact test. Thus, overall ICC–J scores from *T. muris*-infected mice were compared with those of uninfected mice by using the Fisher exact test. Scores were grouped in the 2-way table so that mice that had scores less than or equal to 9 formed one class, and those that had scores greater than or equal to 10 formed the second class. After 2-tailed *P* values were calculated by using the Fisher exact test, the Holm step-down procedure was used to correct for multiple comparisons. The null hypothesis was rejected when the *P* value was less than or equal to 0.05. Spleen scoring data were treated similarly. For the cell-count data, one-way ANOVA followed by the Holm–Sidak correction for multiple comparisons was performed by using SigmaStat 3.1 (Systat Software, San Jose, CA). Statistical null hypotheses were rejected when *P* values were less than or equal to 0.05.

T-RFLP analysis. For experiments 1 and 2, T-RFLP profiles were processed as follows. Only profiles having total area under the curve of at least 10,000 fluorescence units between fragment sizes of 100 and 990 bp were considered. Only OTU with heights greater than or equal to 50 fluorescence units and comprising at least 1% of the total area were included.[18] Only profiles with at least 65% of the total area between 100 and 990 bp accounted for were included. Consensus profiles were produced by T-Align processing of duplicates.[40] Peaks present in less than 5% of the consensus profiles were removed. Two replicates of the T-RFLP analysis were run on each sample to evaluate repeatability. Samples that did not achieve designated peak height and repeatability criteria were not used for statistical analyses.

Hierarchical clustering analysis. The presence or absence, and, if present, the number of OTU was analyzed as a pairwise matrix of similarities where each sample was compared with all others. The Dice similarity measure was used for presence–absence data and the Bray–Curtis similarity measure for abundance data. The resulting matrices were used to construct dendrograms by using unweighted pair group method with arithmetic averaging (UPGMA) using PAST software (version 1.93).[8] In experiment 1, UPGMA clustering was performed on abundance and presence–absence data in experiment 1 on all mice (TLR4-deficient C3BirIL10$^{-/-}$ mice with and without *T. muris* infection and TLR4-deficient IL10 sufficient mice [C3H/HeJ] with and without *T. muris*) and of C3BirIL10$^{-/-}$ mice with and without *T. muris* infection. In experiment 2, UPGMA clustering was performed on abundance and presence–absence data of all 3 groups of mice (noncolitic C3BirIL10$^{-/-}$ mice, colitic C3Bir IL10$^{-/-}$ mice, and noncolitic C3H/HeJ mice) and on noncolitic and colitic C3BirIL10$^{-/-}$ mice. In all cases, the averages of distances between clusters were unweighted by the number of taxa in each cluster at each step, and each distance contributed

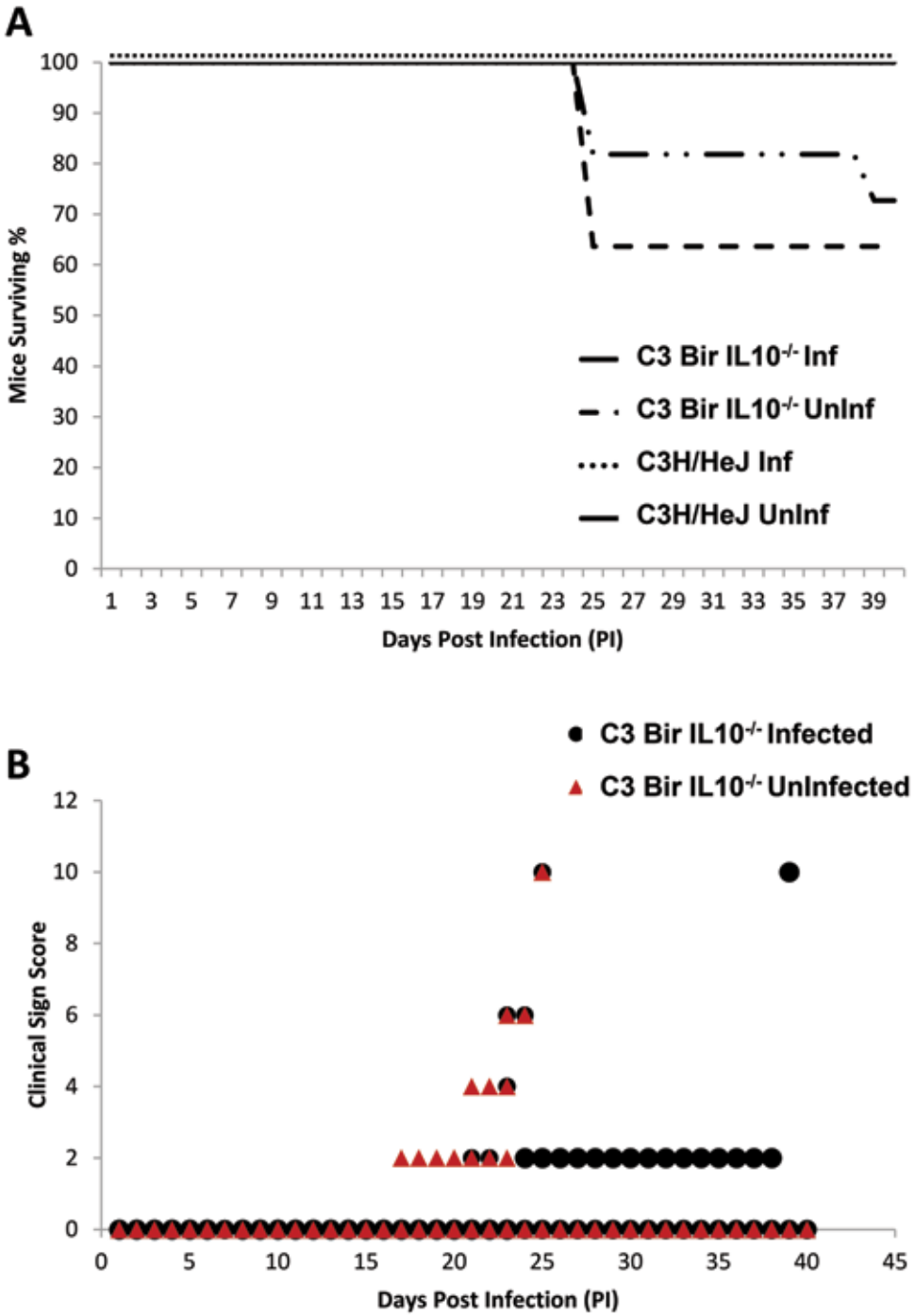

Figure 1. Survival curves and clinical signs of disease in C3Bir IL10$^{-/-}$ and C3H/HeJ mice infected with *T. muris* (Inf) or sham inoculated (Uninf). (A) Survival curves. All mice were infected on day 0 and euthanized as dictated by clinical signs or at day 40 PI. (B) Graded score based on clinical signs of disease in infected and uninfected C3Bir IL10$^{-/-}$ mice. Uninfected C3Bir IL10$^{-/-}$ mice showed clinical signs 4 d earlier than mice of the same genotype infected with *T. muris*; however, mice of both groups were euthanized for the first time at day 25 PI when their clinical scores exceeded a value of 8.

equally to the final result. Results are expressed as a dendrogram with overall similarities among taxa evaluated by bootstrapping.

Nonmetric Multidimensional Scaling (NMDS). In experiment 1, NMDS plots were generated to illustrate variation in the composition and structure of proximal colon microbial communities among 1) all mice in all treatment groups (TLR4-deficient C3Bir IL10$^{-/-}$ mice with and without *T. muris* infection and TLR4-deficient IL10 sufficient mice [C3H/HeJ] with and without *T. muris*); 2) *Trichuris*-infected mice of both genotypes; 3) C3BirIL10$^{-/-}$ mice only (*T. muris*-infected and uninfected); 4) C3H/HeJ mice only (*T. muris*-infected and uninfected); and 5) uninfected mice of both genotypes (C3BirIL10$^{-/-}$ and C3H/HeJ). The Dice similarity measure was used for presence–absence data and the Bray Curtis similarity measure for abundance data. NMDS plots were also made to illustrate variation in abundance data on all 3 groups of mice in Experiment 2 (noncolitic C3Bir IL10$^{-/-}$ mice, colitic C3Bir IL10$^{-/-}$ mice, and noncolitic C3H/HeJ mice).

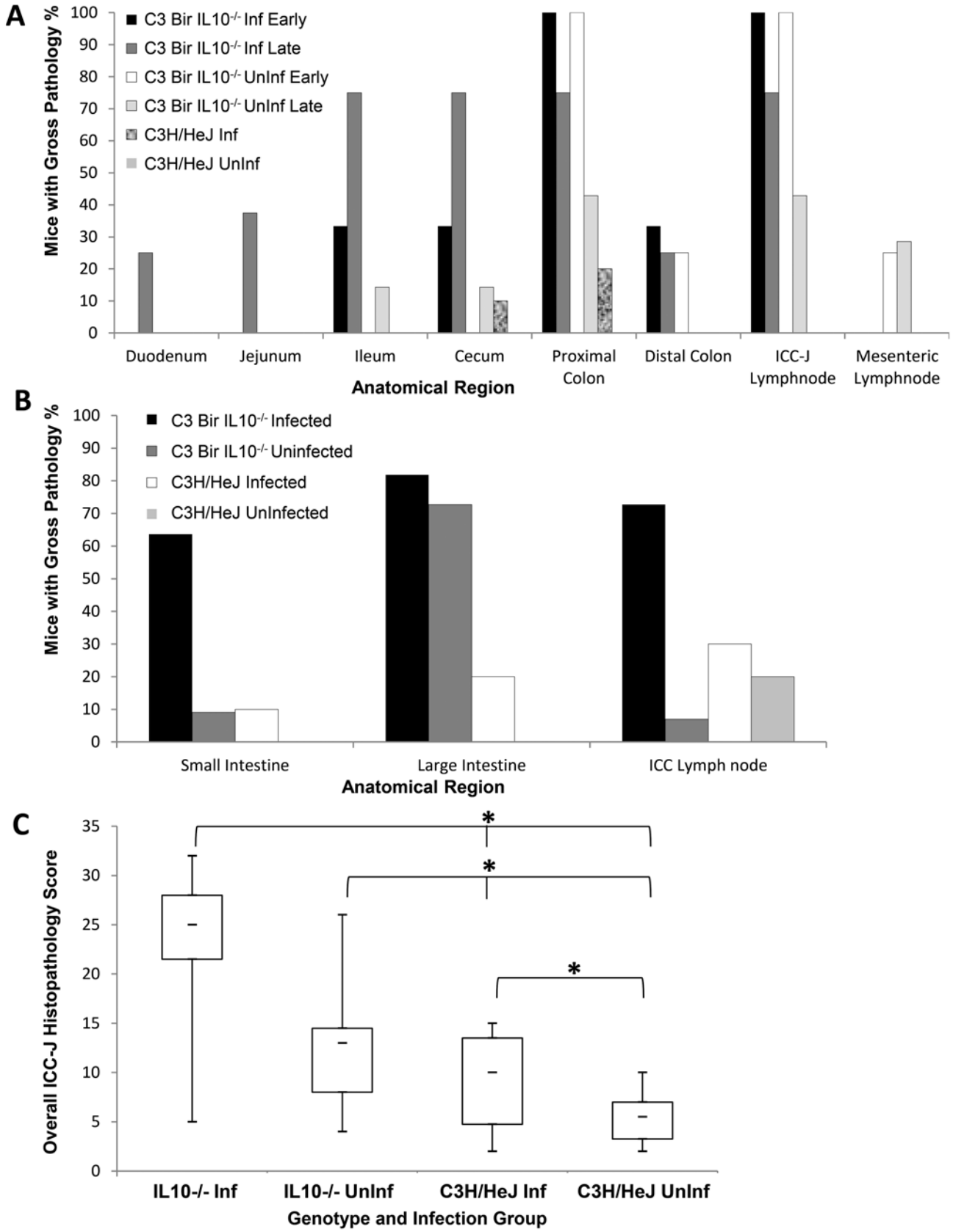

Figure 2. Gross pathology and histologic lesions observed at the time of necropsy; Experiment 1. (A)Distribution of pathology in all compartments of the small and large bowel in both mouse genotypes and infection groups (Infected, Inf; Uninfected, Uninf) divided according to the time of euthanasia (early, prior to 29 d PI; late, day 39 or 40 PI regardless of clinical signs of disease). (B)Percentage of mice with pathology in small and large intestines and lymph nodes in the 4 treatment groups. C3Bir IL10$^{-/-}$ (IL10$^{-/-}$) mice infected with *T. muris* tended to have widespread lesions in the gastrointestinal tract, while uninfected mice of this genotype with spontaneous colitis had gross changes in the colon and

NMDS plots were also made to illustrate variation in the I presence-absence data in mice of these 3 groups. NMDS analyses were then applied to the C3Bir IL10$^{-/-}$ mice alone comparing colitic and noncolitic mice of the same genotype and the normal mice of both genotypes for I abundance and presence-absence.

Software. PAST software (version 1.93)[8] was used to generate dendrograms based on hierarchical clustering and NMDS scatter plots and to conduct ANOSIM and similarity percentage (SIMPER) analyses for assessing which taxa were primarily responsible for the observed differences between the groups of samples.[8] The composition and structure of the microbial communities of mice were compared by using Dice (Sorenson) and Bray–Curtis diversity indices, respectively. In experiment 2, the T-Align program was used to generate consensus T-RFLP profiles from duplicate samples prior to further analysis.[40]

Microbial community analysis (MiCA). MiCA with APLAUS8 was used to identify to name particular 16S fragment sizes based on T-RFLP data.[39] This analysis reports a listing of phylotypes consistent with the observed fragment sizes.

qPCR analysis. In experiment 1, iQ5 PCR detection system software (Bio-Rad) was used to calculate the cycle threshold value for each reaction and the mean cycle threshold value for each set of triplicates. Using the corresponding standard curve, the starting quantity of DNA was calculated for each reaction and the mean starting quantity for the triplicate reactions for each sample. The mice were then grouped according to genotype (IL10$^{+/+}$ or IL10$^{-/-}$) and experimental end-point (early [that is, before day 29] or late [day 39 or 40]). The mean starting quantities of DNA for each mouse within a specific treatment and end-point group were then calculated and compared by using ANOVA. The null hypothesis was rejected when the *P* value was 0.05 or less.

Results

Experimental procedures. The first aim was to describe pathologic manifestations of *T. muris* infection in C3Bir IL10$^{-/-}$ mice and to contrast those manifestations with pathology in both *T. muris*-infected C3H/HeJ mice and in uninfected C3Bir IL10$^{-/-}$ mice experiencing spontaneous colitis. The second aim was to determine whether shifts in composition of proportions of intestinal microbiota were associated with pathologic changes in the gut. In experiment 1, *T. muris*-infected C3H/HeJ IL10$^{-/-}$ were compared with *T. muris*-infected C3H/HeJIL10$^{-/-}$ and uninfected controls of both mouse genotypes. In experiment 2, a larger number of uninfected C3HBirIL10$^{-/-}$ mice with and without spontaneous colitis were compared with each other and with normal C3H/HeJ mice.

Typhlocolitis in *Trichuris*-infected mice. All *T. muris*-infected and some uninfected C3BirIL10$^{-/-}$ mice developed clinical signs of typhlocolitis, with some mice requiring early euthanasia, whereas all C3H/HeJ mice in both the infected and uninfected groups remained disease-free (experiment 1, Figure 1). C3BirIL10$^{-/-}$ mice have been observed to develop spontaneous colitis in multiple laboratories,[37] including our own, despite SPF status. *Trichuris*-infected and uninfected C3Bir IL10$^{-/-}$ mice with severe disease necessitating early euthanasia (Figure 1 A) had clinical signs including hunched posture, decreased activity, rough hair coat, dehydration, and increased frequency and volume of diarrhea (Figure 1 B). Furthermore, some C3Bir IL10$^{-/-}$ mice in both the infected and uninfected groups had severe clinical signs (Figure 1 B). Uninfected C3BirIL10$^{-/-}$ mice that developed spontaneous colitis showed clinical signs 4 d earlier than *T. muris*-infected mice of the same genotype, but both groups progressed to a requirement for euthanasia at the same time (25 d after infection) (Figure 1 A). Three of 11 (0 of 5 female and 3 of 6 male) *T. muris*-infected C3BirIL10$^{-/-}$ mice were euthanized early due to severe clinical signs of disease, whereas 4 of 11 (1 of 6 female and 3 of 5 male) uninfected mice displayed clinical signs requiring early euthanasia (Figure 1 A). Unlike *T. muris*-infected mice, many uninfected C3BirIL10$^{-/-}$ mice that required early euthanasia had severely ulcerated perineal tissues due to chronic watery diarrhea.

Intestinal inflammatory changes in C3BirIL10$^{-/-}$ mice infected with *T. muris*. C3BirIL10$^{-/-}$ mice infected with *T. muris* had severe diffuse inflammatory changes in the gastrointestinal tract as compared with uninfected mice (experiment 1). Specifically, C3Bir IL10$^{-/-}$ mice infected with *T. muris* had inflammation involving a larger portion of the gastrointestinal tract—including the small intestine (starting as proximal as the anterior ileum), the cecum and the proximal colon—compared with uninfected C3Bir IL10$^{-/-}$ mice and C3H/HeJ mice (Figure 2 A and B). In 3 of 11 C3Bir IL10$^{-/-}$ infected mice, the distal colon was also involved. The gross pathologic changes observed in these gastrointestinal tracts included organ distension or enlargement, thickened wall, fluid-filled intestines, and enlarged ICC–J and mesenteric lymph nodes. Infected C3Bir IL10$^{-/-}$ mice that required early euthanasia had lesions in the large bowel, whereas mice surviving longer had widespread gastrointestinal lesions in the small and large intestines. This observation indicates that *Trichuris* lesions apparently started in the large bowel and extended to the entire gastrointestinal tract. This pattern is in contrast to uninfected C3Bir IL10$^{-/-}$ mice with severe lesions of spontaneous colitis, in which lesions were confined to the colon.

ICC–J lesions in response to *Trichuris* (experiment 1). The differences in the overall histopathologic score for all mouse genotypes and infection groups are shown in Figure 2 C. *Trichuris*-infected C3BirIL10$^{-/-}$ mice had higher median ICC–J lesion scores when compared with uninfected C3Bir IL10$^{-/-}$ mice, infected C3H/HeJ mice, and uninfected C3H/HeJ mice; however, statistical analyses showed significant differences only between *Trichuris*-infected C3BirIL10$^{-/-}$ mice and the 2 C3H/HeJ groups (infected, uninfected). Histopathology scores of uninfected C3BirIL10$^{-/-}$ mice were higher ($P \leq 0.001$) than in either *Trichuris*-infected or uninfected C3H/HeJ mice, showing that spontaneous colitis was present in this group. Finally, *Trichuris*-infected C3H/HeJ mice had higher histopathologic lesion scores than uninfected C3H/HeJ mice, showing that mice of this genotype react to infection with this helminth, but did not experience spontaneous colitis under these experimental conditions. One-way ANOVA analysis of these analyses indicated significant ($P \leq 0.001$) differences between the treatment group means.

Although *Trichuris*-infected and uninfected C3BirIL10$^{-/-}$ mice did not differ in their histopathology scores, different immune cell types were present in these 2 groups (Figure 3 and Figure 4). Infected C3BirIL10$^{-/-}$ mice had a predominantly neutrophilic response, particularly seen as exudates in the luminal contents, as compared with uninfected mice C3BirIL10$^{-/-}$ ($P \leq 0.05$) (Figure 4 A). In addition, a significantly ($P \leq 0.0184$) higher percentage

gut associated lymph nodes. More *T. muris* infected C3H/HeJ mice had gross lesions than uninfected mice of this genotype. (C)Histopathologic scoring; boxes enclose central 50% of scores, whiskers indicate maximum and minimum scores; bars within boxes indicate median score; asterisks indicate significant differences.

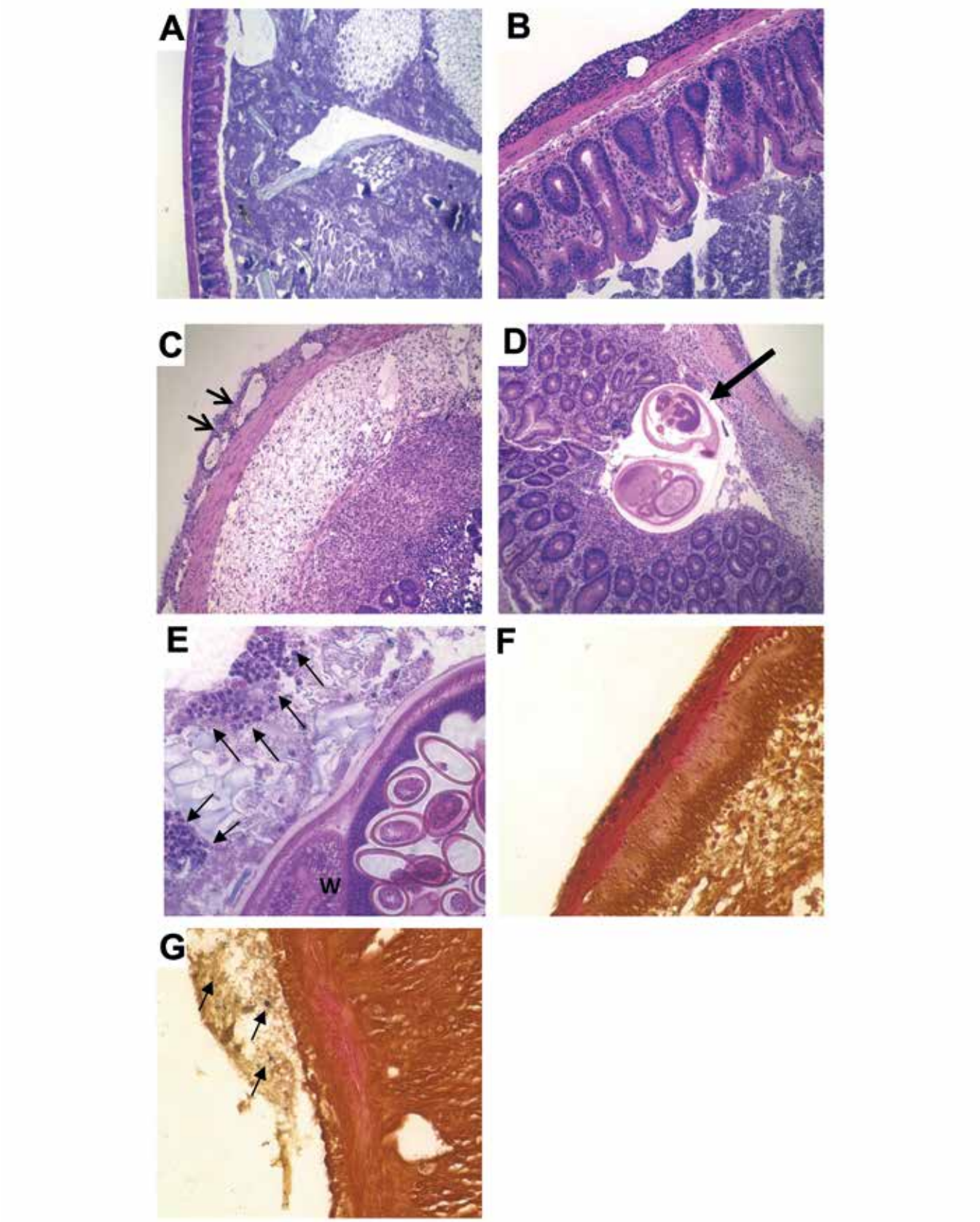

Figure 3. Histology of the ICC–J from mice in Experiment 1. All images were obtained at 20× magnification. A throughE show H and E stained tissue sections, while F andG show Gram stained tissue sections. (A) Normal mouse cecum from uninfected C3H/HeJ mouse. (B) Inflammatory cells present on the serosal side of the cecal tissue in a *T. muris* infected C3Bir IL10$^{-/-}$ mouse (upper left). (C) Inflammatory cells with bacteria on the serosal side of the colon in a *T. muris* infected C3Bir IL10$^{-/-}$ mouse (arrows). Note the marked edema in the submucosa. (D) *T. muris* adult worm under the submucosa of the cecum (arrow) in a *T. muris* infected C3Bir IL10$^{-/-}$ mouse. (E) Neutrophilic exudates surrounding female adult

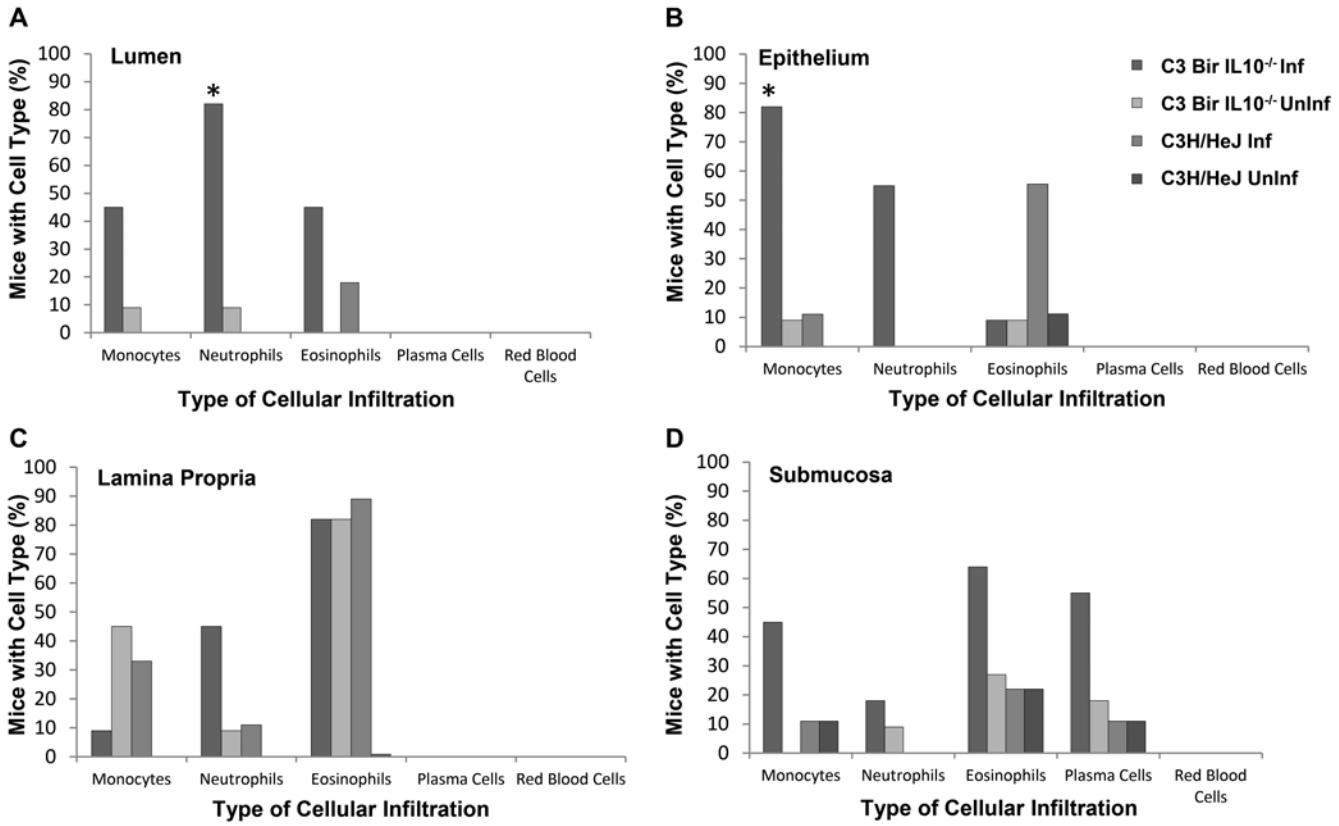

Figure 4. Inflammatory cell types present in the ileocecocolic junctions of mice in Experiment 1. (A)Lumen; (B)Epithelium; (C)Lamina propria; (D)Submucosa. *T. muris* infected C3Bir IL10$^{-/-}$ mice had increased neutrophilic responses in the lumen, epithelium and lamina propria. They also had mononuclear infiltrates in the lumen, epithelium and submucosa. Uninfected mice of the same genotype with spontaneous colitis had mononuclear and eosinophilic responses mainly in the lamina propria. Infected C3H/HeJ mice had mainly eosinophilic infiltrates in the epithelium and lamina propria, while few uninfected mice of this genotype had infiltrating cells in any compartment.

of the *Trichuris*-infected C3Bir IL10$^{-/-}$ infected mice had monocytic infiltrates in the epithelial layer of the ICC–J where the majority of worms reside (Figure 4 B). *Trichuris*-infected and uninfected C3BirIL10$^{-/-}$ mice—some of which had spontaneous colitis—had cellular infiltrates composed of mononuclear cells and eosinophils that were found mainly in the lamina propria Figure 4 C). In these mice, occasional mononuclear cells and neutrophils were present in the lumen of the gut (Figure 4 A). *Trichuris*-infected C3H/HeJ mice had an eosinophilic response in the epithelium, lamina propria, and intestinal lumen that correlated with significantly lower ICC–J lesion scores, as compared with *Trichuris*-infected C3Bir IL10$^{-/-}$ mice (Figure 4 A through C). Many *Trichuris*-infected C3BirIL10$^{-/-}$ mice also had eosinophils, but they were located mainly in the submucosa along with monocytes and plasma cell infiltrates (Figure 4 D).

Extraintestinal bacteria and peritonitis in *Trichuris*-infected C3BirIL10$^{-/-}$ mice. Assessment of histopathologic lesions revealed extraintestinal bacteria and signs of peritonitis in *Trichuris*-infected C3BirIL10$^{-/-}$ mice (experiment 1). Assessment of stained histologic sections of the ICC–J showed signs of inflammation and bacteria on the serosal side of the tissues in some *T. muris*-infected C3BirIL10$^{-/-}$ mice (Figure 3 B through D). Mice in this group had monocytic inflammatory cells adherent to the serosal side of the intestinal tissue with or without detectable bacteria in the inflammatory exudates (Figure 3 B and C). To further confirm the presence of bacteria in these locations, Gram stains were performed on tissue sections from the same mice; gram-positive rods were seen among the inflammatory exudates on the serosal sides of 7 of the 11 (64%) ICC–J sections (Figure 3 G). Mature adult *T. muris* worms were observed in close association with neutrophilic inflammatory exudates within the colonic lumen in 9 of the 11 infected C3Bir IL10$^{-/-}$ mice (Figure 3 E). In addition, in one of these mice, a cross-section of a mature *Trichuris* worm was present beneath the submucosa (Figure 3 D).

Enlarged spleens in *T. muris*-infected C3Bir IL10$^{-/-}$ mice and C3Bir IL10$^{-/-}$ mice with spontaneous colitis. The spleens of C3H/HeJ and C3Bir IL10$^{-/-}$ *T. muris*-infected mice and uninfected C3Bir IL10$^{-/-}$ mice that developed spontaneous colitis were enlarged as compared with those of uninfected mice (experiment 1). In experiment 1, spleens were weighed at necropsy and the spleen:body weight ratio calculated (Figure 5 A). A section of splenic tissue was evaluated histologically for the size of the periarteriolar lymphatic sheaths and amount of extramedullary hematopoietic tissue. The only statistically significant differences in these parameters were found between the infected C3Bir IL10$^{-/-}$ and C3H/HeJ mice and between the infected C3Bir IL10$^{-/-}$ and uninfected C3H/HeJ mice (one-way ANOVA, $P \leq 0.001$). The splenic tissue of infected C3Bir IL10$^{-/-}$ mice was not significantly different from uninfected mice of the same genotype, many of which had spontaneous colitis (Figure 5 B). Significant differences in histologic scores were present in

T. muris worm (W) in the lumen of a C3Bir IL10$^{-/-}$ mouse cecum (arrows). (F) ICC–J section of an uninfected C3Bir IL10$^{-/-}$ normal mouse. Note smooth serosal surface free of bacteria and inflammation (left side). (G) ICC–J of a *T. muris* infected C3Bir IL10$^{-/-}$ mouse with Gram-positive rods (arrows) among the inflammatory cells on the serosal side of the cecum.

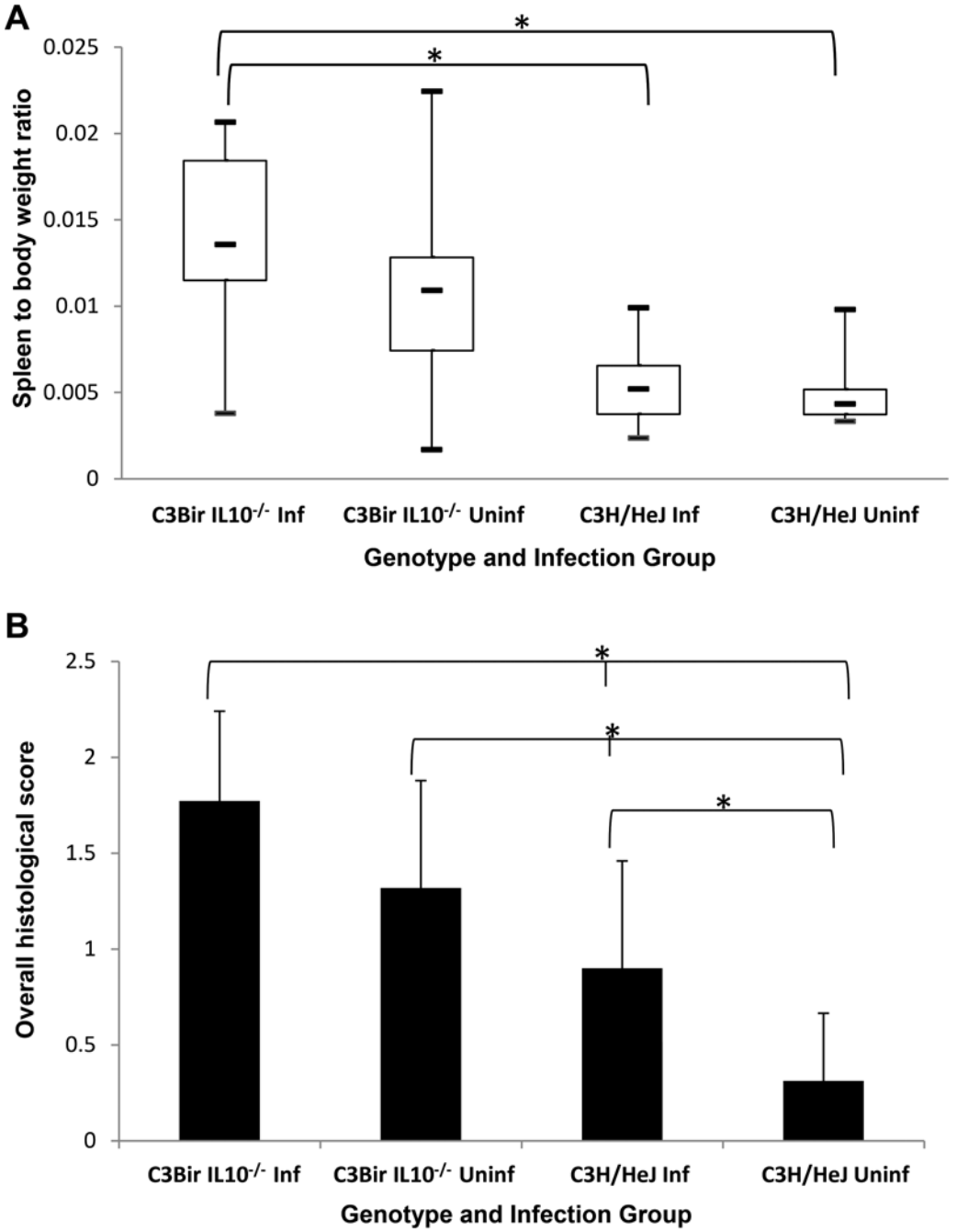

Figure 5. Spleen weights and histopathologic lesions from mice in Experiment 1. (A)Spleen to body weight ratios of mice in the 4 treatment groups, *T. muris* infected C3Bir IL10$^{-/-}$ mice (IL10$^{-/-}$ Inf), uninfected C3Bir IL10$^{-/-}$ mice (Il10$^{-/-}$ Uninf), *T. muris* infected C3H/HeJ mice and uninfected C3H/HeJ mice (Infected, Inf; Uninfected, Uninf). Statistically significant differences were noted between the C3Bir IL10$^{-/-}$ infected and C3H/HeJ infected mice and this group and the C3H/HeJ uninfected mice (one-way ANOVA, $P \leq 0.001$). (B)Histopathologic lesion scores of spleens from mice in the 4 treatment groups in Experiment 1 revealed statistically significant differences (one-way ANOVA, $P < 0.001$) between all groups except C3Bir IL10$^{-/-}$ infected and uninfected mice. Thus, spleen weights and lesions were increased either with *Trichuris* infection or spontaneous colitis in C3Bir IL10$^{-/-}$ mice. Infected C3H/HeJ mice had increased histologic scores in spleen compared with uninfected mice of this genotype, but no differences in spleen to body weight ratios.

comparisons between infected and uninfected C3H/HeJ mice, between infected C3Bir IL10$^{-/-}$ mice and all other groups, except for uninfected mice of the same genotype, and between uninfected C3Bir IL10$^{-/-}$ mice and both infected and uninfected C3H/HeJ mice (one-way ANOVA, $P \leq 0.001$). These data show that spontaneous colitis or infection with *Trichuris* in these strains of mice is associated with enlargement of the splenic periarteriolar lymphatic sheaths and increased extramedullary hematopoiesis.

Spontaneous colitis in C3BirIL10$^{-/-}$ but not C3H/HeJ mice. In experiment 2, 34 of the 75 (45%) uninfected C3Bir IL10$^{-/-}$ colony-housed mice developed spontaneous colitis, as evidenced by clinical signs (diarrhea, hunched posture, diminished movement) and histopathologic scoring of the ICC–J, whereas C3H/HeJ mice did not (Figure 6 A through E). Stained sections of

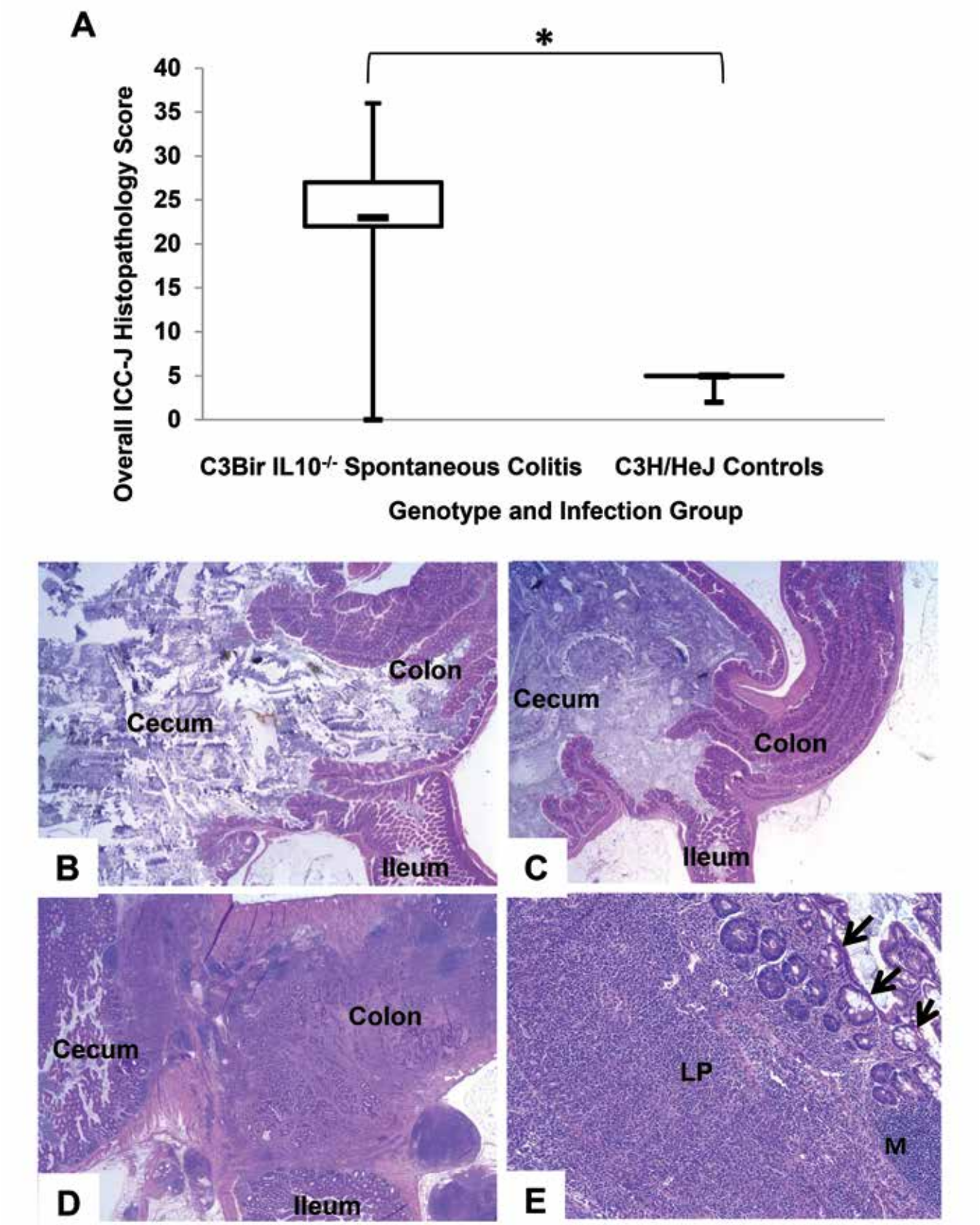

Figure 6. Histology of the ileocecocolic junction from mice in Experiment 2 from a specific-pathogen free colony with and without spontaneous colitis. (A)Histopathologic scoring; boxes enclose central 50% of scores, whiskers indicate maximum and minimum scores; bars within boxes indicate median score; asterisks indicate significant differences. Images B through D were obtained at 2× magnification and image E was taken at 10× magnification. Images are as follows: (B)Normal ICC–J from C3Bir IL10$^{-/-}$ mouse; (C)Normal ICC–J from C3H/HeJ mouse, (D)ICC–J from a C3Bir IL10$^{-/-}$ mouse with spontaneous colitis, and Panel E: Higher power view of ICC–J from C showing the mononuclear cell infiltrates (M) in the lamina propria (LP). Arrows show the villus tip of the epithelium.

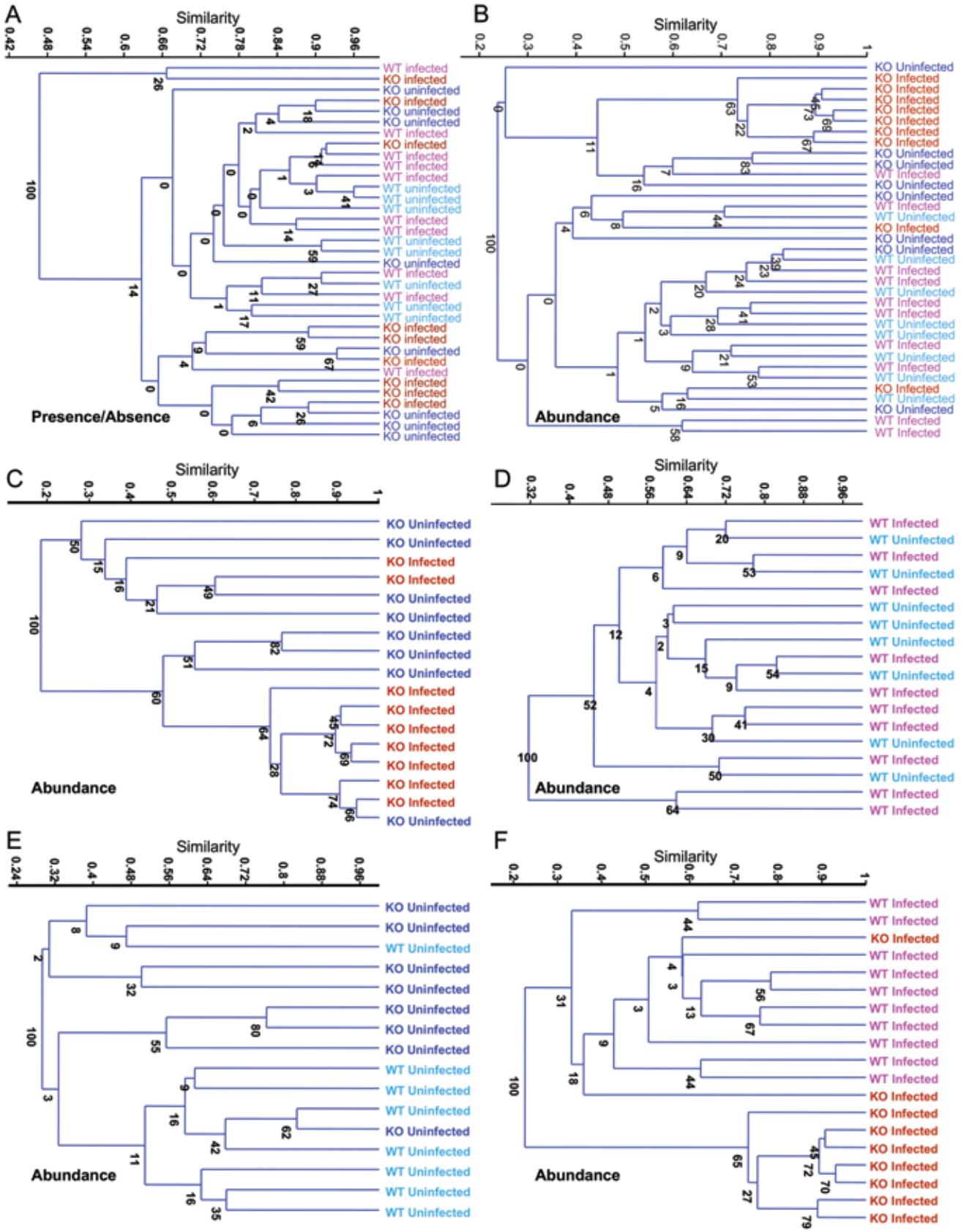

Figure 7. Hierarchical clustering of T-RFLP data from Experiment 1. Bootstrap support for all nodes is given as percent of 1000 replicates. C3BirIL10$^{-/-}$ indicated by KO and C3H/HeJ indicated by WT. (A)Dendrogram for OTU presence/ absence data for all mice; Dice similarity measure; UPGMA clustering. (B) Dendrogram for OTU abundance data for all mice; Bray–Curtis similarity measure; UPGMA clustering. (C) Dendrogram for abundance data for infected and uninfected C3Bir IL10$^{-/-}$ (KO) mice; Bray–Curtis similarity measure; UPGMA clustering. (D) Dendrogram for abundance data for infected and uninfected C3H/HeJ (WT) mice; Bray–Curtis similarity measure; UPGMA clustering. (E)

the ICC–J of mice with colitis show substantial cellular infiltrates in the lamina propria (Figure 6 D and E) as compared with noncolitic C3Bir IL10$^{-/-}$ (Figure 6 B) and C3H/HeJ (Figure 6 C) colony-housed mice. However, 5 of the 18 (28%) uninfected C3H/HeJ mice had enlarged ICC–J lymph nodes, which is often the first gross lesion of colitis seen in this model.[26] The 34 C3Bir IL10$^{-/-}$ mice with spontaneous colitis ranged in age from 7 to 29 wk, whereas the 41 spontaneous-colitis–free mice of this genotype ranged from 8 to 23 wk. The 5 C3H/HeJ mice with enlarged ICC–J lymph nodes ranged in age from 16 to 29 wk, whereas the 13 mice of this genotype with no signs of inflammation ranged from 9 to 26 wk. Regardless of the small differences in the age ranges of the different groups of mice, the histologic scores of the entire group of C3H/HeJ mice ranged from 2 to 5, which is within the normal range and indicated that no colitis lesions were present. Spontaneous colitis occurred in the C3Bir IL10$^{-/-}$ mice despite housing in a barrier facility and extensive testing that revealed no known viruses, colitogenic bacteria, or parasites present.

Microbial communities in mice of experiment 1. In both experiments 1 and 2, samples available from all mice in all experimental groups provided adequate T-RFLP data to conduct multivariate hierarchical classification (clustering), ordination (NMDS), and ANOSIM to be conducted, based on the criteria described in the Materials and Methods section.

Results of analyses of T-RFLP patterns obtained for mice in experiment 1 are shown in Figures 7 and 8 and Table 4. Distinct clustering of mice based on OTU presence was not observed with regard to genotype or infection status (Figure 7 A), but relative abundance of OTUs were significantly different in infected C3Bir IL10$^{-/-}$ mice (Figure 7 B). Moreover, the 2 clusters that had 100% bootstrap support had different proportions of the mouse genotypes represented. One cluster consisted of a single C3H/HeJ mouse and 11 C3Bir IL10$^{-/-}$ mice, including 7 of the 9 infected C3Bir IL10$^{-/-}$ mice for which acceptable T-RFLP patterns were obtained. The second cluster contained 6 C3Bir IL10$^{-/-}$ mice and 17 C3H/HeJ mice. Therefore, according to cluster analysis of the entire data set, both mouse genotype and infection status appear to contribute to differences in the relative abundance of microbial community members.

Presence–absence data did not reveal any apparent clustering by infection status in C3Bir IL10$^{-/-}$ mice (data not shown), but infected and uninfected C3Bir IL10$^{-/-}$ mice clustered based on the relative abundance of OTU (Figure 7 C). Infected and uninfected C3H/HeJ mouse OTU did not show clustering by either presence–absence (data not shown) or relative abundance (Figure 7 D). Data from uninfected C3Bir IL10$^{-/-}$ mice and uninfected C3H/HeJ mice and from infected C3Bir IL10$^{-/-}$ mice and infected C3H/HeJ mice were analyzed separately by hierarchical clustering to examine the effect of mouse genotype on the response of the microbial community to *T. muris* infection. Clustering of abundance data by mouse genotype in abundance data was apparent in both analyses. In uninfected mice, one of the 2 clusters having 100% bootstrap support was composed of 4 C3Bir IL10$^{-/-}$ mice and a single C3H/HeJ mouse, whereas the other was composed of 4 C3Bir IL10$^{-/-}$ mice and 7 C3H/HeJ mice (Figure 7 E). The effect appeared to be stronger in infected mice: one of the 2 clusters having 100% bootstrap support was composed of 2 C3Bir IL10$^{-/-}$ mice and all 10 C3H/HeJ mice, whereas the other was solely composed of the remaining 7 C3Bir IL10$^{-/-}$ mice (Figure 7 F).

Hierarchical clustering results were confirmed by independent parallel analyses with NMDS (Figure 8); this analysis also yielded associations not seen in the clustering results. In the NMDS scatter plot for presence–absence data in all infected and uninfected mice of both genotypes, (Figure 8 A), most (15 of 18) C3H/HeJ mice fell on the positive side of the coordinate 1 axis (pink and aqua triangles), whereas the majority (11 of 17) of C3Bir IL10$^{-/-}$ mice fell on the negative side (red and blue squares), regardless of infection status. Hierarchical clustering did not reveal this separation in presence–absence by genotype. NMDS analysis of relative abundance (Figure 8 B) gave similar results, with (15 of 18) C3H/HeJ mice falling on the positive side of the coordinate 1 axis (pink and aqua triangles) and 11 of the 17 C3Bir IL10$^{-/-}$ mice on the negative side (red and blue squares).

NMDS scatter plots of presence–absence data from infected and uninfected C3Bir IL10$^{-/-}$ mice and from infected and uninfected C3H/HeJ mice did not display strong separation between infected and uninfected mice of either genotype in presence–absence (data not shown). In accordance with the results of hierarchical clustering, NMDS analysis of abundance data showed separation in relative abundance between infected and uninfected C3Bir IL10$^{-/-}$ mice (Figure 8 C) but not between infected and uninfected C3H/HeJ mice (Figure 8 D). The influence of mouse genotype on relative abundance is confirmed by NMDS analysis of uninfected mice of both genotypes (Figure 8 E) and infected mice of both genotypes (Figure 8 F).

ANOSIM analyses were used to test the significance of the effects revealed by the clustering and NMDS analyses. In experiment 1, 2-way ANOSIM analysis indicated that microbial communities in the proximal colons of infected and uninfected C3Bir IL10$^{-/-}$ and C3H/HeJ mice differed both qualitatively and quantitatively. Two-way ANOSIM analysis of OTU presence–absence data for all mice by using the Dice similarity measure revealed differences in community composition due to mouse genotype (ANOSIM $P = 0.0004$, R = 0.2444; the low R value indicates a relatively weak effect) but not infection status (ANOSIM $P = 0.5400$, R = –0.0092) in this data set. Two-way ANOSIM analysis of OTU abundance data for all mice by using the Bray–Curtis similarity measure revealed significant differences in community structure due to both genotype (ANOSIM $P = 0.0002$, R = 0.4051) and infection status (ANOSIM $P = 0.0265$, R = 0.1358).

Posthoc comparisons of OTU presence–absence data for *Trichuris*-infected and uninfected C3Bir IL10$^{-/-}$ and infected and uninfected C3H/HeJ mice did not reveal any differences in presence–absence due to infection status. Posthoc comparisons of OTU abundance data for infected and uninfected C3Bir IL10$^{-/-}$ and infected and uninfected C3H/HeJ mice showed a significant difference in relative abundance due to infection status for C3Bir IL10$^{-/-}$ mice ($P = 0.0048$ and R = 0.3099), but not for infected and uninfected C3H/HeJ mice ($P = 0.6545$, R = –0.0384). The ANOSIM results thus confirm the hierarchical clustering and NMDS outcomes for these comparisons.

Posthoc comparisons of OTU presence-absence data for uninfected C3Bir IL10$^{-/-}$ and uninfected C3H/HeJ mice revealed differences in both presence–absence and the relative abundance

Dendrogram for abundance data for uninfected C3Bir IL10$^{-/-}$ mice (KO) and uninfected C3H/HeJ mice (WT); Bray–Curtis similarity measure; UPGMA clustering. (F)Dendrogram for abundance data for infected C3Bir IL10$^{-/-}$ (KO) mice and infected C3H/HeJ (WT) mice; Bray-Curtis similarity measure; UPGMA clustering.

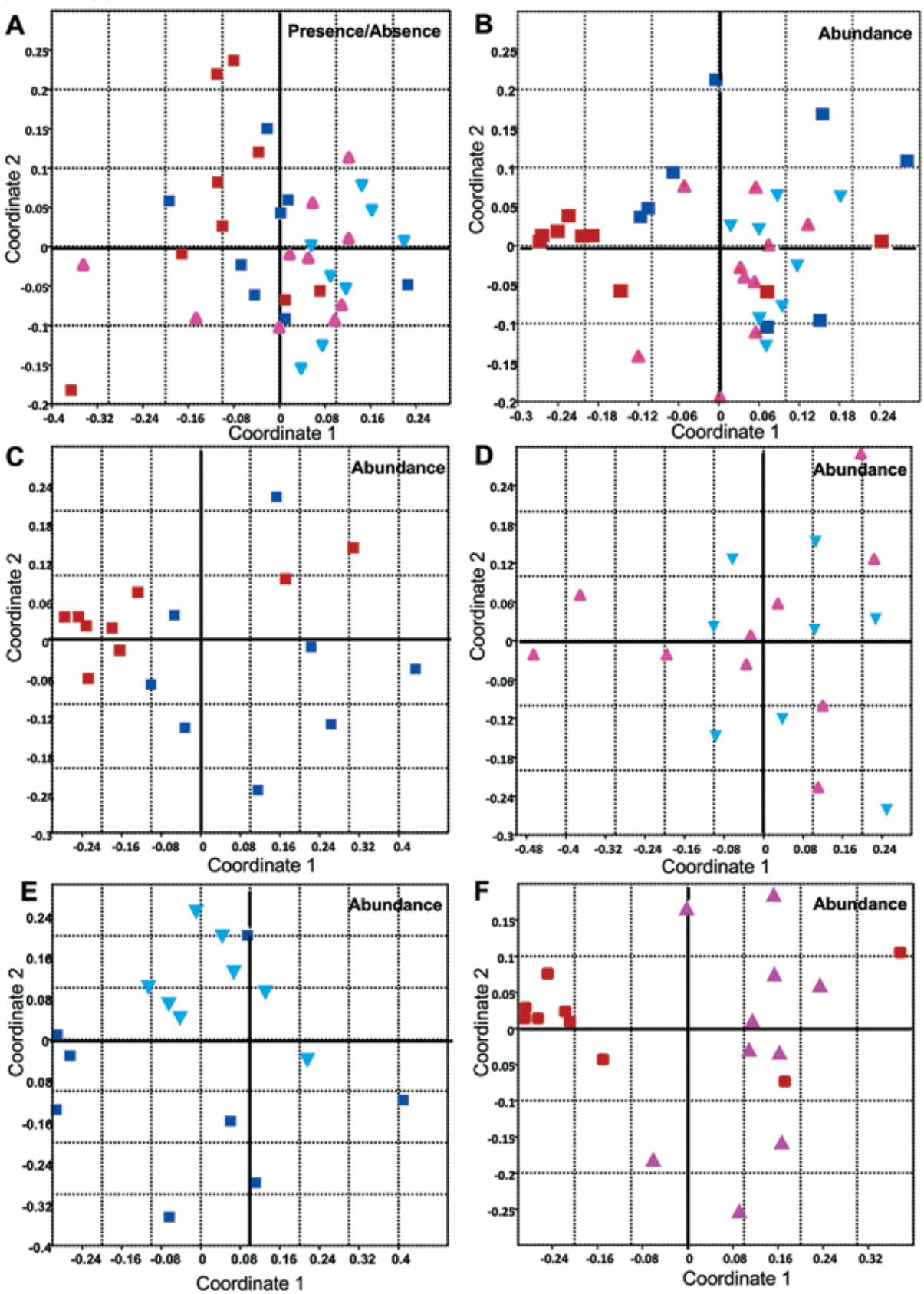

Figure 8. Nonmetric multidimensional scaling plots (NMDS) analysis of T-RFLP data from Experiment 1. (A)NMDS plot for OTU presence/absence data for all mice; Dice similarity measure; *T. muris* infected C3Bir IL10$^{-/-}$ mice (red squares), uninfected C3Bir IL10$^{-/-}$ mice (blue squares), *T. muris* infected C3H/HeJ mice (pink triangles), and uninfected C3H/HeJ mice (aqua triangles). (B)NMDS plot for OTU abundance data for all mice; Bray–Curtis similarity measure; *T. muris* infected C3Bir IL10$^{-/-}$ mice (red squares), uninfected C3Bir IL10$^{-/-}$ mice (blue squares), *T. muris* infected C3H/HeJ mice (pink triangles), and uninfected C3H/HeJ mice (aqua triangles). (C)NMDS plot for abundance data for infected and

Table 4. Summary of UPGMA, NMDS, and ANOSIM analyses of Experiment 1 T-RFLP data. Dominant groupings and significant ANOSIM results are shown in bold type. Bootstrap support ≥ 50% and $P \leq 0.05$ considered significant.

Groups compared		Major UPGMA clusters		Discreet NMDS clusters	ANOSIM	
Mouse genotype	**Infection status**	**Cluster 1**	**Cluster 2**		**Presence/absence of taxa**	**Relative abundance of taxa**
Community composition (presence/absence of taxa)						
Both (Figure 7 A)	Both (Figure 7 A)	No significant clustering	No significant clustering	**Separation by genotype** (coordinate 1)	Two-way ANOSIM: **Genotype, *P* = 0.0004;** Infection status, NS	NA
Community structure (relative abundance of taxa)						
Both (Figure 7 B)	Both (Figure 7 B)	0 uninfected C3H/HeJ	**8 uninfected C3H/HeJ**	**Infected C3 Bir IL10$^{-/-}$**	NA	Two-way ANOSIM: **Genotype, *P* = 0.0002; Infection status, *P* = 0.0265**
		1 infected C3H/HeJ	**9 infected C3H/HeJ**			
		4 uninfected C3 Bir IL10$^{-/-}$	4 uninfected C3 Bir IL10$^{-/-}$			
		7 infected C3 Bir IL10$^{-/-}$	2 infected C3 Bir IL10$^{-/-}$			
C3 Bir IL10$^{-/-}$ only (Figure 7 C)	Both (Figure 7 C)	4 uninfected C3 Bir IL10$^{-/-}$	4 uninfected C3 Bir IL10$^{-/-}$	**Infected C3 Bir IL10$^{-/-}$**	One-way ANOSIM (infection status): NS	One-way ANOSIM, (infection status): ***P* = 0.0048**
		2 infected C3 Bir IL10$^{-/-}$	**7 infected C3 Bir IL10$^{-/-}$ with significant subclustering of infected mice**			
C3H/HeJ (Figure 7 D)	Both (Figure 7 D)	No significant clustering (2 infected outliers)	No significant clustering (2 infected outliers)	None	One-way ANOSIM (infection status): NS	One-way ANOSIM, (infection status): NS
Both (Figure 7 E)	Uninfected only (Figure 7 E)	1 uninfected C3H/HeJ	**7 uninfected C3H/HeJ**	**Uninfected C3H/HeJ**	One-way ANOSIM, (genotype): ***P* = 0.0075**	One-way ANOSIM, (genotype): ***P* = 0.0264**
		4 uninfected C3 Bir IL10$^{-/-}$	4 uninfected C3 Bir IL10$^{-/-}$			
Both (Figure 7 F)	Infected only (Figure 7 F)	0 infected C3H/HeJ	**10 infected C3H/HeJ**	**Infected C3 Bir IL10$^{-/-}$**	One-way ANOSIM, (genotype): NS	One-way ANOSIM, (genotype): ***P* = 0.0004**
		7 infected C3 Bir IL10$^{-/-}$	2 infected C3 Bir IL10$^{-/-}$			

of community members due to mouse genotype (presence–absence, $P = 0.0075$ and R = 0.3457; abundance, $P = 0.0264$ and R = 0.2757). Posthoc comparisons of OTU abundance data for infected C3Bir IL10$^{-/-}$ and infected C3H/HeJ mice indicated a significant difference in community structure due to mouse genotype ($P = 0.0004$ and R = 0.5344) but not in community composition (presence–absence, $P = 0.1418$, R = 0.1431).

SIMPER analyses showed that a single OTU, which we termed 'taxon P,' was responsible for 53/66 = 80% of the average dissimilarity between the microbial communities of *Trichuris*-infected and uninfected C3 Bir IL10$^{-/-}$ mice. Previous work[29] suggests that this OTU may correspond to a *Clostridium* species. In an attempt to identify members of the microbial community that were responsible for the differences noted with T-RFLP, MiCA analysis and species-specific qPCR assays were performed for *Clostridium* groups I and XIV, *Bacteroides* spp., and *E. coli*.

For experiment 1, MiCA analysis performed on taxon P did not yield a clear taxonomic assignment for this taxon (fragment size, 983 to 996 bp); possibilities included a number of enteric bacteria: *Clostridium*, Eubacterium, *Lachnospira*, *Fusibacter*, and several members of the Enterobacteriaceae. DNA suitable for qPCR analysis was available from a total of 9 infected and uninfected C3Bir IL10$^{-/-}$ mice and 8 infected and uninfected C3H/HeJ mice. qPCR did not reveal significant differences in *Bacteroides* spp., *E. coli*, or *Clostridium* groups I and XIV between infected C3H/HeJ and C3Bir IL10$^{-/-}$ mice and their uninfected controls (Figure 9). Although no significant changes in the specific bacteria were detected by our species-specific qPCR analyses, 2 general patterns emerged. Specifically, the C3H/HeJ and C3Bir IL10$^{-/-}$ groups of *Trichuris*-infected mice both tended to have lower amounts of *Clostridium* group I and *Bacteroides* spp. in the proximal colon. *Clostridium* group XIV and *E. coli* assays were performed, but no patterns were evident (data not shown).

Microbial communities in mice of experiment 2. No significant differences in abundance or presence–absence of OTU were detected between colitic and noncolitic C3Bir IL10$^{-/-}$ mice and

uninfected C3Bir IL10$^{-/-}$ mice; Bray–Curtis similarity measure; *T. muris* infected (red squares) and uninfected (blue squares) C3Bir IL10$^{-/-}$ mice. Panel D: NMDS plot for abundance data for infected and uninfected C3H/HeJ mice; Bray-Curtis similarity measure; *T. muris* infected (pink triangle) and uninfected (aqua triangles) C3H/HeJ mice. Panel E: NMDS plot for abundance data for uninfected C3Bir IL10$^{-/-}$ mice and uninfected C3H/HeJ mice; Bray–Curtis similarity measure; Uninfected C3Bir IL10$^{-/-}$ mice (blue squares) and uninfected C3H/HeJ mice (aqua triangles). (F) NMDS plot for abundance data for infected C3Bir IL10$^{-/-}$ mice and infected C3H/HeJ mice; Bray-Curtis similarity measure; Infected C3Bir IL10$^{-/-}$ mice (red squares) and infected C3H/HeJ mice (pink triangles).

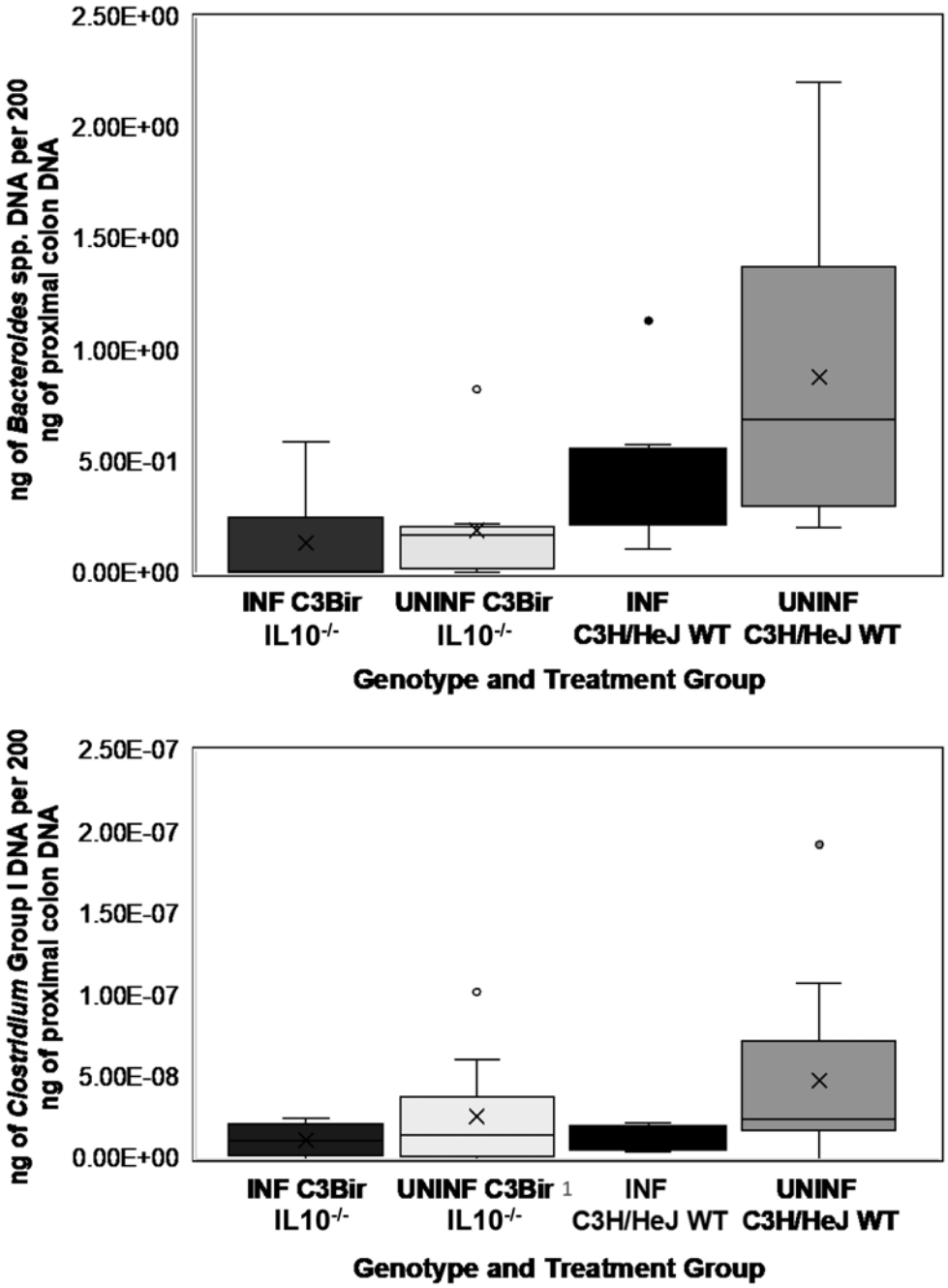

Figure 9. Quantitative Real Time PCR (QPCR) for major bacterial groups shown as box plots. (A) *Bacteriodes-Prevotella-Porphyromonas* group; (B) *Clostridium* group I. Tukey rule was used to define outliers in these analyses. qPCR did not reveal significant differences in *Bacteroides* spp., *E. coli* spp., or *Clostridium* Groups I and XIV spp. between C3H/HeJ and C3Bir IL10$^{-/-}$ infected mice and their uninfected controls

noncolitic C3H/HeJ mice raised in an SPF colony (experiment 2). Results of analyses of T-RFLP patterns obtained for mice in experiment 2 are shown in Figure 10.

None of the dendrograms or NMDS plots show any grouping by genotype or by presence or absence of colitis in the gastrointestinal tract. One-way ANOSIM analysis was significant for presence–absence data (community composition: $P = 0.0457$, R = 0.0637), but no posthoc comparisons between groups were significant after correction for multiple comparisons. In addition, one-way ANOSIM analysis was not significant for abundance data (community structure: $P = 0.1184$, R = 0.0267).

In experiment 2, SIMPER analysis showed that 3 main contributors—T-RFLP fragments of approximately 365, 489, and 974 bp—to the statistically significant difference between C3H/HeJ WT and colitic C3Bir IL10$^{-/-}$ mice. MiCA analysis of the 3 identified fragment sizes showed that the 365-bp fragment corresponded to several *Prevotella* species, a few bacteria belonging to the *Bacteroidetes*, and many uncultured bacteria, including both human and mouse intestinal bacteria. The 489-bp fragment did not correspond closely to any entries; it corresponded most closely to fragment sizes of 488 and 490 bp, both of which have been reported for uncultured *Ruminococcaceae* bacteria, among many others. The 973-bp fragment corresponded most closely to the 973- and 974-bp fragments that have been reported for

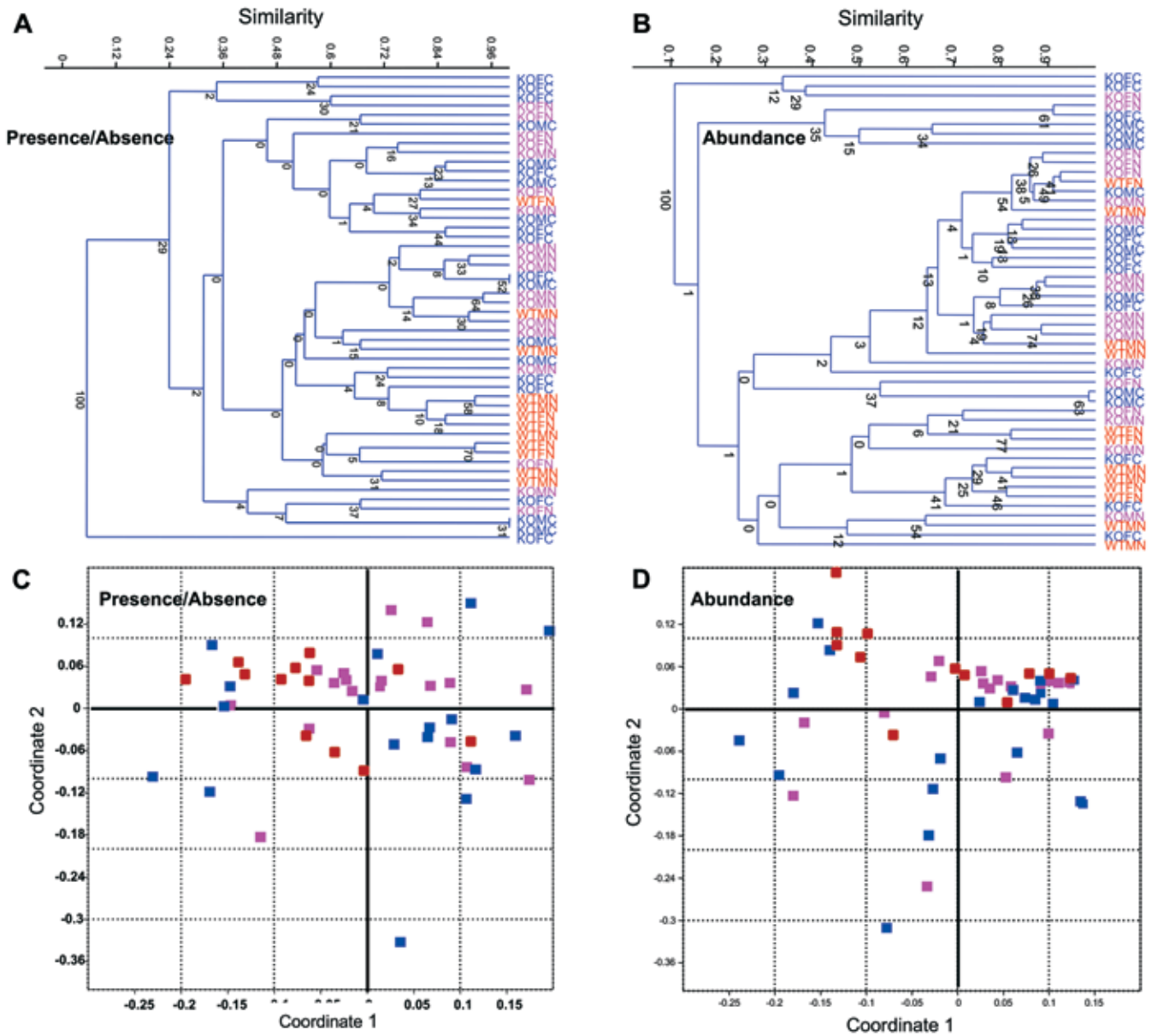

Figure 10. Hierarchical clustering analysis of T-RFLP data from Experiment 2 showing no significant differences in abundance or presence/absence of OTUs between colitic and noncolitic C3Bir IL10$^{-/-}$ mice and noncolitic C3H/HeJ mice raised in a SPF colony. Bootstrap support for all nodes is given as percent of 1000 replicates. KOC (blue) indicates C3BirIL10$^{-/-}$ mice with colitis, KON (pink) indicates C3BirIL10$^{-/-}$ mice without evidence of colitis (normal), WTN (red) indicates C3H/HeJ mice without evidence of colitis. (A)Dendrogram for OTU presence/absence data for all mice; Dice similarity measure; UPGMA clustering. (B)Dendrogram for OTU abundance data for all mice; Bray–Curtis similarity measure; UPGMA clustering. (C)NMDS plot for OTU presence/absence data for all mice; Dice similarity measure; UPGMA clustering. (D)NMDS plot for OTU abundance data for all mice; Bray–Curtis similarity measure; UPGMA clustering.

uncultured marine bacteria. Thus, MiCA analysis did not provide identification of any of the 3 peaks identified by the SIMPER analysis as accounting for the difference between the C3H/HeJ and colitic C3BirIL10$^{-/-}$ mice.

Discussion

We hypothesized that *Trichuris muris*-infected mice would have altered colon microbiota compared with uninfected mice. To test our hypothesis, we infected C3Bir IL10$^{-/-}$ and C3H/HeJ mice with 100 embryonated *Trichuris* eggs and compared them to sham inoculated congenic controls at the time of patency. Both mouse strains were deficient in Toll-like receptor-4 (TLR4) and contain the cytokine deficiency colitis susceptibility-1 (*cdcs*-1) allele. C3Bir IL10$^{-/-}$ mice infected with *T. muris* had significantly different microbial communities in the proximal colon than did uninfected controls. However, the composition and structure of the microbiota did not differ significantly between uninfected C3Bir IL10$^{-/-}$ mouse groups with and without colitis. To further pursue the effect of spontaneous colitis on the composition and structure of microbiota, we assessed proximal colon microbiota of C3Bir IL10$^{-/-}$ mice with and without spontaneous colitis in our breeding colony and compared these microbial communities to those of C3H.HeJ mice that did not develop spontaneous colitis. When colon microbiota OTUs of all colitic mice in this second experiment were compared with noncolitic mice, no statistically significant differences were found between the groups. This work supports our hypothesis that mice infected with *T.*

muris develop distinct microbial communities in the colon, and that these alterations cannot be solely attributed to the presence of inflammation in the gastrointestinal tract.

We examined the effects of the nematode *T. muris* on the host microbial community in its definitive site in the proximal colon of the inbred mouse strains C3H/HeJ and the IL10 deficient C3Bir.129P2(B6). Unlike many lumen dwelling helminths, *Trichuris* has intimate associations with the cecal and colonic epithelium, initiated by penetration of the mucosal barrier as first-stage larvae. This is followed by conditioning of the enteric environment by a complex set of activities from the worms. Therefore, we expect that this worm has community-wide interactions with enteric bacteria. We wanted to test this hypothesis in mouse models of colitis, because *Trichuris* has been shown to interact with particular enteric bacteria[25] and, in some studies, to decrease symptoms of inflammatory bowel disease in exposed patients.[42,43] However, this model was chosen to examine effects on the microbial communities of the proximal colon in mice with various immune system defects (TLR4, IL10, Cdcs1) on a common genetic background and not as a treatment model for IBD in which deficiencies in IL10 would prevent development of the full effects of the worms. Our results support the hypothesis that mice infected with *T. muris* develop distinct colonic microbial communities. However, the shift observed in the microbial community was significantly different from that of uninfected controls in C3Bir IL10$^{-/-}$ mice, but not in C3H/HeJ mice. This difference was observed despite the fact that we assayed the microbial communities at the peak of the *Trichuris* infection at (40 d after inoculation), when many adult worms were present in the proximal colon. This observation suggests that the shifts in the microbial community due to *Trichuris* infection were also influenced by host background genes. These alterations cannot be solely attributed to the presence of inflammation of the tissues, because uninfected C3Bir IL10$^{-/-}$ mice that developed spontaneous colitis had microbial communities similar to those of noncolitic mice of the same genotype. This result also suggests that IL10 and the cells producing it play a key role in shaping proximal colon microbial communities. In fact, *Bacteroides fragilis* and *Faecalibacterium prausnitzii* have been shown to modulate IL10 and to mediate a decrease in colonic inflammation.[28,41] Mice in our colony are monitored for colitogenic bacteria and were negative for *Helicobacter* spp., *Campylobacter* spp., *Citrobacter rodentium*, and *Enterococcus faecalis*. They were also negative for *Faecalibacterium prausnitzii*, which was shown to protect against inflammation.[32] Exploration of presence of probiotic bacteria such as *Bacteroides fragilis* might help to explain the inflammation in these models.

Our studies demonstrated that *T. muris* infection of C3Bir IL10$^{-/-}$ mice that have a spontaneous mutation in TLR4, and the *cdcs-1* colitis susceptibility allele stimulated a significant intestinal inflammatory response. This response led to severe clinical signs of disease that required early euthanasia of some mice, but not at a higher proportion than in uninfected mice of the same genotype that developed spontaneous colitis. Thus, both *Trichuris* infected and uninfected C3Bir IL10$^{-/-}$ mice developed colitis, but mice infected with *Trichuris* took longer to develop clinically apparent colitis. Furthermore, the distribution of the lesions varied between these 2 groups of mice. *Trichuris* infected C3Bir IL10$^{-/-}$ mice had lesions in both the small and large intestine, while C3Bir IL10$^{-/-}$mice with spontaneous colitis had lesions only in the large intestine. We also observed some sex related differences in disease and lesions in C3Bir IL10$^{-/-}$ mice given *Trichuris*. Males appeared to be more susceptible to the adverse effects of *T. muris,* with more male mice experiencing severe clinical signs and a higher death rate. This susceptibility difference has been reported previously for other nematode infections.[46] The presence of *Trichuris* and bacteria outside of the intestinal tract in mice of this genotype occurred in 7 of the 11 knockout mice, which is consistent with the established role of IL10 in resistance to this nematode.[36] We also assessed the effect of *T. muris* infection on IL10 sufficient C3H/HeJ mice, a closely matched background genotype. These mice developed a less severe inflammatory response to the helminth in the colon with only subclinical disease and no deaths. Experiment 1 also examined effects on the spleen because earlier trials demonstrated that mice lacking TLR4 have higher levels of enteric bacteria in the circulation and spleen.[26] Our experiments with *Trichuris* infected mice suggest that the worms may have had anti-inflammatory activity that could have reduced spleen reactivity in *Trichuris* infected C3H/HeJ mice; this phenomenon did not occur in the absence of IL10 in the C3Bir IL10$^{-/-}$ mice. This possibility could also explain why uninfected C3H/HeJ mice also had enlarged spleens.

We also used T-RFLP OTUs to demonstrate that *T. muris* infected C3Bir IL10$^{-/-}$ mice have colonic microbial communities that differ structurally from the uninfected controls. Like 16S rRNA gene sequencing, T-RFLP OTUs correspond to fragments from different bacteria and are an inexpensive means of assessing complex populations with numbers of unculturable bacteria.[23] A number of likely candidates may mediate these changes. For example, the ESP of *Trichuris* fourth-stage larvae and adults have been previously reported to have broad spectrum antibiotic activities,[1,2] which could provide a rapid mechanism for change in the microbiota. *T. suis* also enhanced *C. jejuni* infections in gnotobiotic[25] and SPF pigs.[27] In both of these studies, the presence of the worm increased mucus production, which is known to enhance growth of this bacterium.[15] In addition, in some mice, *T. muris* infections have been reported to induce significant inflammatory responses[36] that have been reported to alter colonic conditions and potentially affect which members of the community predominate. 16S rRNA gene sequencing and metabolomics followed by metagenomic sequencing combined with culturomics of the proximal colon could identify the bacterial species that mainly contribute to pathologic changes seen in infected C3Bir IL10$^{-/-}$ mice.

Our findings indicate that the T-RFLP OTUs of C3Bir IL10$^{-/-}$ mice that developed severe spontaneous colitis did not differ significantly from uninfected C3Bir IL10$^{-/-}$ mice that did not develop spontaneous colitis. ANOSIM analyses of mice when grouped based on histopathologic lesion scores at the ICC–J (data not shown) did not find a significant difference between the mice with inflammation compared with those without inflammation, regardless of infection group, other than those differences seen due to *Trichuris* infection status.

SIMPER analyses showed that a single OTU was responsible for 53% of the 66% average dissimilarity between the microbial communities of *Trichuris* infected and uninfected C3 Bir IL10$^{-/-}$ mice. Because previous work[29] suggests that this OTU may correspond with *Clostridium* spp., qPCR assays were performed for *Clostridium* Group I, *Clostridium* Group XIV, *Bacteroides* spp. and *E. coli*. The abundance of *Clostridium* Group I and *Bacteroides* spp. DNA in *Trichuris* infected mice did not reach the 0.05 cutoff for significance. Larger group sizes and metagenomic sequencing from the proximal colon could better identify which organisms differed between the 2 groups. In a study of pigs infected with *T. suis,* the investigators noted a significant reduction in the abundance of *Fibrobacter* and *Ruminococcus* in the colon microbiota.[45] Although porcine gastrointestinal physiology is different

from that of immune deficient mice, it is tempting to speculate that our OTU fragment sizes of 488.63 and 490.01 may correspond with uncultured colonic bacteria. This could represent a similar effect of *Trichuris* associated with a change in the fibrinolytic capacity of the colon microbiota. The same investigators correlated microbial community changes in *T. suis* infected pigs with metabolomic changes in the colon.[22] They demonstrated decreases in cofactors for carbohydrate and lysine biosynthesis and increased oleic acid by measuring volatile organic compounds in colon contents; these changes were associated with increased inflammation as compared with the uninfected control pigs. A similar metabolomic approach in our mouse models would be interesting because of the differences due to *T. muris* infection, IL10 deficiency and mouse genetic background.

To further assess effects of colitis on colon microbial communities, TLR4 deficient colitis susceptible mice were followed over time in a SPF barrier breeding facility to document development of spontaneous colitis and to compare the composition and structure of their microbial communities with mice of the isogenic strain without colitis. The microbial communities of mice with colitis did not have different structures or compositions from those of isogenic mice without lesions. Although the range of ages of mice in this study (up to 29 wk) was greater than that in Experiment 1, the conclusions did not change when only colony-housed mice between the ages of 8 and 18 wk were included in the analyses (data not shown). Taken together, results of these 2 experiments suggest that the changes observed in the microbial community in *Trichuris* infected mice were specific to the parasitic infection, rather than simply the effect of acute or chronic inflammation in local tissues. These data may also suggest that long standing inflammation cause changes in the microbiota, a phenomenon observed in humans with IBD.[6]

This study has several limitations and suggests areas for future directions. Although our work identified differences in the intestinal microbial communities of mice that were or were not infected with *T. muris* , we were unable to determine which specific microbial community members were responsible for these differences. This information will be useful for determining the potential role for *Trichuris* spp. in health and disease. These differences could be better assessed using sequence-based technologies that identify bacterial groups to the genus level.

Despite this limitation, we believe our study design we used was adequate to test our hypothesis. We recognize that microbial communities can vary significantly between individuals, even in inbred mice kept in the same colony and fed the same diet.[7] This fact has necessitated the use of longitudinal study designs in which an individual is resampled and used as its own control. This type of design permits smaller sample sizes and the use of principle component analysis.[44] Our goals in this work were different. We chose to use large sample sizes of 10 mice per group in a cross-sectional design, with careful control of housing, pathogen status, and diet with the goal of revealing major differences between treatment groups, if they were present. Thus, the differences we found in the microbial community of *Trichuris* infected mice as compared with other treatment groups demonstrated here is robust and consistent with previous studies[22] that show interactions of this helminth with specific microbiotic community members. Thus, we were able to demonstrate that the microbial community structure differed in the *T. muris* infected C3Bir IL10$^{-/-}$ mice as compared with uninfected congeners, even when their gastrointestinal lesions were similar. Overall, this work supports our hypothesis that mice infected with *T. muris* develop distinctive microbial communities in the colon, and that these alterations cannot be solely attributed to the presence of inflammation in the gastrointestinal tract.

Acknowledgments

This project was funded in whole with federal funds from the NCRR, NIH, Department of Health and Human Services, under grant number 5K26RR023080. Mice for experiment 2 were produced by using federal funds from the NIAID, NIH, Department of Health and Human Services, under contract no. N01-AI-30058. While finishing this work, Jamie J Kopper was supported for one semester by a dissertation fellowship grant from the Michigan State University Graduate School through the College of Veterinary Medicine.

All applicable international, national, and institutional guidelines for the care and use of animals were followed.

References

1. **Abner SR, Hill DE, Turner JR, Black ED, Bartlett P, Urban JF, Mansfield LS.** 2002. Response of intestinal epithelial cells to *Trichuris suis* excretory-secretory products and the influence on *Campylobacter jejuni* invasion under in vitro conditions. J Parasitol **88:**738–745.
2. **Abner SR, Parthasarathy G, Hill DE, Mansfield LS.** 2001. *Trichuris suis*: detection of antibacterial activity in excretory-secretory products from adults. Exp Parasitol **99:**26–36. https://doi.org/10.1006/expr.2001.4643.
3. **American Veterinary Medical Association.** 2020. American veterinary medical association guidelines for the euthanasia of animals: 2020 ed, Schaumburg (IL): American Veterinary Medical Association.
4. **Beckwith J, Cong Y, Sundberg JP, Elson CO, Leiter EH.** 2005. Cdcs1, a major colitogenic locus in mice, regulates innate and adaptive immune response to enteric bacterial antigens. Gastroenterology **129:**1473–1484. https://doi.org/10.1053/j.gastro.2005.07.057.
5. **Farmer MA, Sundberg JP, Bristol IJ, Churchill GA, Li R, Elson CO, Leiter EH.** 2001. A major quantitative trait locus on chromosome 3 controls colitis severity in IL-10-deficient mice. Proc Natl Acad Sci USA **98:**13820–13825. https://doi.org/10.1073/pnas.241258698.
6. **Frank DN, St Amand AL, Feldman RA, Boedeker EC, Harpaz N, Pace NR.** 2007. Molecular-phylogenetic characterization of microbial community imbalances in human inflammatory bowel diseases. Proc Natl Acad Sci USA **104:**13780–13785. https://doi.org/10.1073/pnas.0706625104.
7. **Friswell MK, Gika H, Stratford IJ, Theodoridis G, Telfer B, Wilson ID, McBain AJ.** 2010. Site and strain-specific variation in gut microbiota profiles and metabolism in experimental mice. PLoS One **5:**1–9. https://doi.org/10.1371/journal.pone.0008584.
8. **Hammer O, Harper DAT, Ryan PD.** [Internet]. 2001. PAST: PAleontological STatistics Software Version 065 Oslo Univ, Oslo. [Cited 21 October 2020]. Available at: https://palaeo-electronica.org/2001_1/past/past.pdf.
9. **Hayes KS, Bancroft AJ, Goldrick M, Portsmouth C, Roberts IS, Grencis RK.** 2010. Exploitation of the intestinal microflora by the parasitic nematode *Trichuris muris*. Science **328:**1391–1394. https://doi.org/10.1126/science.1187703.
10. **Hill DE, Gamble HR, Rhoads ML, Fetterer RH, Urban JF Jr.** 1993. *Trichuris suis*: a zinc metalloprotease from culture fluids of adult parasites. Exp Parasitol **77:**170–178. https://doi.org/10.1006/expr.1993.1074.
11. **Hill DE, Romanowski RD, Urban JF Jr.** 1997. A *Trichuris* specific diagnostic antigen from culture fluids of *Trichuris suis* adult worms. Vet Parasitol **68:**91–102. https://doi.org/10.1016/S0304-4017(96)01055-2.
12. **Hill DE, Sakanari JA.** 1997. *Trichuris suis*: thiol protease activity from adult worms. Exp Parasitol **85:**55–62. https://doi.org/10.1006/expr.1996.4125.
13. **Holm JB, Sorobetea D, Kiilerich P, Ramayo-Caldas Y, Estelle J, Ma T, Madsen L, Kristiansen K, Svensson-Frej M.** 2015. Chronic *Trichuris muris* infection decreases diversity of the intestinal microbiota and concomitantly increases the abundance of lactobacilli. PLoS One **10:**1–22. https://doi.org/10.1371/journal.pone.0125495.
14. **Houlden A, Hayes KS, Bancroft AJ, Worthington JJ, Wang P, Grencis RK, Roberts IS.** 2015. Chronic *Trichuris muris* infection in

C57BL/6 mice causes significant changes in host microbiota and metabolome: effects reversed by pathogen clearance. PLoS One **10:**1–25. https://doi.org/10.1371/journal.pone.0125945.

15. **Hugdahl MB, Beery JT, Doyle MP.** 1988. Chemotactic behavior of *Campylobacter jejuni*. Infect Immun **56:**1560–1566. https://doi.org/10.1128/IAI.56.6.1560-1566.1988.
16. **Institute for Laboratory Animal Research.** 2011. Guide for the care and use of laboratory animals, 8th ed. Washington (DC): National Academies Press.
17. **Khan IU, Gannon V, Kent R, Koning W, Lapen DR, Miller J, Neumann N, Phillips R, Robertson W, Topp E, van Bochove E, Edge TA.** 2007. Development of a rapid quantitative PCR assay for direct detection and quantification of culturable and non-culturable *Escherichia coli* from agriculture watersheds. J Microbiol Methods **69:**480–488. https://doi.org/10.1016/j.mimet.2007.02.016.
18. **Kitts CL.** 2001. Terminal restriction fragment patterns: a tool for comparing microbial communities and assessing community dynamics. Curr Issues Intest Microbiol **2:**17–25.
19. **Kopper JJ, Mansfield LS.** 2010. Development of improved methods for delivery of Trichuris muris to the laboratory mouse. Parasitol Res **107:**1103–1113. https://doi.org/10.1007/s00436-010-1978-8.
20. **Kopper JJ, Patterson JS, Mansfield LS.** 2015. Metronidazole-but not IL-10 or prednisolone-rescues *Trichuris muris* infected C57BL/6 IL-10 deficient mice from severe disease. Vet Parasitol **212:**239–252. https://doi.org/10.1016/j.vetpar.2015.07.038.
21. **Lee TD, Wright KA.** 1978. The morphology of the attachment and probable feeding site of the nematode *Trichuris muris* (Schrank, 1788) Hall, 1916. Can J Zool **56:**1889–1905. https://doi.org/10.1139/z78-258.
22. **Li RW, Wu S, Li W, Navarro K, Couch RD, Hill D, Urban JF Jr.** 2012. Alterations in the porcine colon microbiota induced by the gastrointestinal nematode *Trichuris suis*. Infect Immun **80:**2150–2157. https://doi.org/10.1128/IAI.00141-12.
23. **Liu WT, Marsh TL, Cheng H, Forney LJ.** 1997. Characterization of microbial diversity by determining terminal restriction fragment length polymorphisms of genes encoding 16S rRNA. Appl Environ Microbiol **63:**4516–4522. https://doi.org/10.1128/AEM.63.11.4516-4522.1997.
24. **Mansfield LS, Bell JA, Wilson DL, Murphy AJ, Elsheikha HM, Rathinam VA, Fierro BR, Linz JE, Young VB.** 2007. C57BL/6 and congenic interleukin-10-deficient mice can serve as models of *Campylobacter jejuni* colonization and enteritis. Infect Immun **75:**1099–1115. https://doi.org/10.1128/IAI.00833-06.
25. **Mansfield LS, Gauthier DT, Abner SR, Jones KM, Wilder SR, Urban JF.** 2003. Enhancement of disease and pathology by synergy of *Trichuris suis* and *Campylobacter jejuni* in the colon of immunologically naive swine. Am J Trop Med Hyg **68:**70–80. https://doi.org/10.4269/ajtmh.2003.68.70.
26. **Mansfield LS, Patterson JS, Fierro BR, Murphy AJ, Rathinam VA, Kopper JJ, Barbu NI, Onifade TJ, Bell JA.** 2008. Genetic background of IL-10$^{-/-}$ mice alters host-pathogen interactions with *Campylobacter jejuni* and influences disease phenotype. Microb Pathog **45:**241–257. https://doi.org/10.1016/j.micpath.2008.05.010.
27. **Mansfield LS, Urban JF Jr.** 1996. The pathogenesis of necrotic proliferative colitis in swine is linked to whipworm induced suppression of mucosal immunity to resident bacteria. Vet Immunol Immunopathol **50:**1–17. https://doi.org/10.1016/0165-2427(95)05482-0.
28. **Mazmanian SK, Round JL, Kasper DL.** 2008. A microbial symbiosis factor prevents intestinal inflammatory disease. Nature **453:**620–625. https://doi.org/10.1038/nature07008.
29. **Nagashima K, Hisada T, Sato M, Mochizuki J.** 2003. Application of new primer-enzyme combinations to terminal restriction fragment length polymorphism profiling of bacterial populations in human feces. Appl Environ Microbiol **69:**1251–1262. https://doi.org/10.1128/AEM.69.2.1251-1262.2003.
30. **Panesar TS.** 1981. The early phase of tissue invasion by *Trichuris muris* (nematoda: Trichuroidea). Z Parasitenkd **66:**163–166. https://doi.org/10.1007/BF00925723.
31. **Parthasarathy G, Mansfield LS.** 2005. *Trichuris suis* excretory secretory products (ESP) elicit interleukin-6 (IL-6) and IL-10 secretion from intestinal epithelial cells (IPEC-1). Vet Parasitol **131:**317–324. https://doi.org/10.1016/j.vetpar.2005.03.043.
32. **Quévrain E, Maubert MA, Michon C, Chain F, Marquant R, Tailhades J, Miquel S, Carlier L, Bermúdez-Humarán LG, Pigneur B, Lequin O, Kharrat P, Thomas G, Rainteau D, Aubry C, Breyner N, Afonso C, Lavielle S, Grill JP, Chassaing G, Chatel JM, Trugnan G, Xavier R, Langella P, Sokol H, Seksik P.** 2016. Identification of an anti-inflammatory protein from *Faecalibacterium prausnitzii*, a commensal bacterium deficient in Crohn's disease. Gut **65:**415–425. http://dx.doi.org/10.1136/gutjnl-2014-307649.
33. **Rhoads ML, Fetterer RH, Hill DE, Urban JF Jr.** 2000. *Trichuris suis*: a secretory chymotrypsin/elastase inhibitor with potential as an immunomodulator. Exp Parasitol **95:**36–44. https://doi.org/10.1006/expr.2000.4502.
34. **Rinttilä T, Kassinen A, Malinen E, Krogius L, Palva A.** 2004. Development of an extensive set of 16S rDNA-targeted primers for quantification of pathogenic and indigenous bacteria in faecal samples by real-time PCR. J Appl Microbiol **97:**1166–1177. https://doi.org/10.1111/j.1365-2672.2004.02409.x.
35. **Rutter JM, Beer RJ.** 1975. Synergism between *Trichuris suis* and the microbial flora of the large intestine causing dysentery in pigs. Infect Immun **11:**395–404. https://doi.org/10.1128/IAI.11.2.395-404.1975.
36. **Schopf LR, Hoffmann KF, Cheever AW, Urban JF Jr, Wynn TA.** 2002. IL-10 is critical for host resistance and survival during gastrointestinal helminth infection. J Immunol **168:**2383–2392. https://doi.org/10.4049/jimmunol.168.5.2383.
37. **Sellon RK, Tonkonogy S, Schultz M, Dieleman LA, Grenther W, Balish E, Rennick DM, Sartor RB.** 1998. Resident enteric bacteria are necessary for development of spontaneous colitis and immune system activation in interleukin-10-deficient mice. Infect Immun **66:**5224–5231. https://doi.org/10.1128/IAI.66.11.5224-5231.1998.
38. **Sestak K, Merritt CK, Borda J, Saylor E, Schwamberger SR, Cogswell F, Didier ES, Didier PJ, Plauche G, Bohm RP, Aye PP, Alexa P, Ward RL, Lackner AA.** 2003. Infectious agent and immune response characteristics of chronic enterocolitis in captive rhesus macaques. Infect Immun **71:**4079–4086. https://doi.org/10.1128/IAI.71.7.4079-4086.2003.
39. **Shyu C, Soule T, Bent SJ, Foster JA, Forney LJ.** 2007. MiCA: a web-based tool for the analysis of microbial communities based on terminal-restriction fragment length polymorphisms of 16S and 18S rRNA genes. Microb Ecol **53:**562–570. https://doi.org/10.1007/s00248-006-9106-0.
40. **Smith CJ, Danilowicz BS, Clear AK, Costello FJ, Wilson B, Meijer WG.** 2005. T-Align, a web-based tool for comparison of multiple terminal restriction fragment length polymorphism profiles. FEMS Microbiol Ecol **54:**375–380. https://doi.org/10.1016/j.femsec.2005.05.002.
41. **Sokol H, Pigneur B, Watterlot L, Lakhdari O, Bermudez-Humaran LG, Gratadoux JJ, Blugeon S, Bridonneau C, Furet JP, Corthier G, Grangette C, Vasquez N, Pochart P, Trugnan G, Thomas G, Blottiere HM, Dore J, Marteau P, Seksik P, Langella P.** 2008. *Faecalibacterium prausnitzii* is an anti-inflammatory commensal bacterium identified by gut microbiota analysis of Crohn disease patients. Proc Natl Acad Sci USA **105:**16731–16736. https://doi.org/10.1073/pnas.0804812105.
42. **Summers RW, Elliott DE, Urban JF Jr, Thompson R, Weinstock JV.** 2005. *Trichuris suis* therapy in Crohn's disease. Gut **54:**87–90. https://doi.org/10.1136/gut.2004.041749.
43. **Summers RW, Elliott DE, Urban JF Jr, Thompson RA, Weinstock JV.** 2005. *Trichuris suis* therapy for active ulcerative colitis: a randomized controlled trial. Gastroenterology **128:**825–832. https://doi.org/10.1053/j.gastro.2005.01.005.
44. **Wang M, Ahrné S, Antonsson M, Molin G.** 2004. T-RFLP combined with principal component analysis and 16S rRNA gene sequencing: an effective strategy for comparison of fecal microbiota in infants of different ages. J Microbiol Methods **59:**53–69. https://doi.org/10.1016/j.mimet.2004.06.002.
45. **Wu S, Li RW, Li W, Beshah E, Dawson HD, Urban JF Jr.** 2012. Worm burden-dependent disruption of the porcine colon microbiota by *Trichuris suis* infection. PLoS One **7:**1–9. https://doi.org/10.1371/journal.pone.0035470.
46. **Zuk M, McKean KA.** 1996. Sex differences in parasite infections: patterns and processes. Int J Parasitol **26:**1009–1023. https://doi.org/10.1016/S0020-7519(96)80001-4.